Aus der Klinik für Neurochirurgie

der Heinrich-Heine-Universität Düsseldorf

Direktorin: Prof. Dr. med. Katharina Faust

Rapalink-1 Attenuates Smoke Condensate-Induced Vascular Senescence and SASP in Vascular Cells

Dissertation

zur Erlangung des Grades eines Doktors der Medizin

der Medizinischen Fakultät der Heinrich-Heine-Universität Düsseldorf

vorgelegt von

Jinliang You

Düsseldorf, 2026

As an inaugural dissertation printed by permission of the

Faculty of Medicine at Heinrich Heine University Düsseldorf

Signed:

Dean: Prof. Dr. Nikolaj Klöcker

First examiner: Prof. Dr. Sajjad Muhammad

Second examiner: PD Dr. Marius Kaschner

Parts of this work have been published:

You, J., Liu, H., Khan, D., Muhereza, R., Faust, K., & Muhammad, S. (2026). Smoke Condensate-Induced Vascular Senescence and SASP Are Attenuated by Dual mTORC1/2 Inhibition with Rapalink-1. International Journal of Molecular Sciences, 27(8), 3636. doi:10.3390/ijms27083636.

Zusammenfassung

Rauchen ist ein führender vermeidbarer Risikofaktor für kardiovaskuläre und zerebrovaskuläre Erkrankungen. Es fördert die Gefäßalterung durch oxidativen Stress, Entzündungsreaktionen und Umbauprozesse der extrazellulären Matrix (ECM). Zelluläre Seneszenz könnte einen Mechanismus darstellen, der Rauchbelastung mit langfristigen Gefäßschäden verbindet. Seneszente Endothelzellen und glatte Gefäßmuskelzellen (SMCs) können zur endothelialen Dysfunktion, proinflammatorischen Signalgebung und strukturellen Schwächung der Gefäßwand beitragen.

Zur Untersuchung dieser Prozesse wurde Tabakrauchkondensat (SC) als In-vitro-Modell verwendet. In der vorliegenden Arbeit wurde untersucht, ob Rapalink-1, ein dualer mTORC1/2-Inhibitor, SC-induzierte Veränderungen in humanen Nabelschnurvenen-Endothelzellen (HUVECs) und vaskulären SMCs abschwächt. Die SC-Exposition war in beiden Zelltypen mit erhöhten oxidativen Stress-readouts, einer Akkumulation von DNA-Schadensmarkern und seneszenzassoziierten Veränderungen verbunden, darunter erhöhte SA-β-gal-Aktivität, verminderte Lamin-B1-Expression und erhöhte p21-Expression. Diese Veränderungen gingen mit Merkmalen einher, die mit einem seneszenzassoziierten sekretorischen Phänotyp (SASP) und ECM-Umbau vereinbar sind. Rapalink-1 schwächte mehrere SC-induzierte Reaktionen ab. Die Behandlung reduzierte die oxidationssensitive Fluoreszenz und die Akkumulation von DNA-Schadensmarkern, schwächte seneszenzassoziierte Readouts ab und normalisierte ausgewählte inflammatorische sowie matrixbezogene Genexpressionsveränderungen teilweise. Auf Signalebene war SC mit erhöhten NF-κB-, MAPK- und nachgeschalteten mTOR-bezogenen Readouts verbunden, während Rapalink-1 mehrere dieser signalassoziierten Reaktionen reduzierte.

Zusammenfassend schwächte Rapalink-1 zentrale Komponenten der SC-induzierten vaskulären Stressantwort in vitro ab. Diese Befunde unterstützen weitere Untersuchungen zur Rolle mTOR-bezogener Signalwege als regulatorische Mechanismen bei rauchbedingter vaskulärer Schädigung und vaskulärer Alterung.

Summary

Smoking is a leading preventable risk factor for cardiovascular and cerebrovascular disease. It promotes vascular aging through oxidative stress, inflammation, and extracellular matrix (ECM) remodeling. Cellular senescence may represent one mechanism linking smoke exposure to long-term vascular damage. Senescent endothelial cells and vascular smooth muscle cells (SMCs) can contribute to endothelial dysfunction, pro-inflammatory signaling, and structural weakening of the vessel wall.

To investigate these processes, tobacco smoke condensate (SC) was used as an in vitro model. The present study examined whether Rapalink-1, a dual mTORC1/2 inhibitor, attenuates SC-induced changes in human umbilical vein endothelial cells (HUVECs) and vascular SMCs. SC exposure was associated with increased oxidative stress-associated readouts, DNA damage marker accumulation, and senescence-associated changes in both cell types, including increased SA-β-gal activity, reduced Lamin B1 expression, and elevated p21 expression. These changes were accompanied by features consistent with a senescence-associated secretory phenotype (SASP) and ECM remodeling. Rapalink-1 attenuated several SC-induced responses. Treatment reduced oxidation-sensitive fluorescence and DNA damage-associated marker accumulation, attenuated senescence-associated readouts, and partially normalized selected inflammatory and matrix-related gene expression changes. At the signaling level, SC was associated with increased NF-κB-, MAPK-, and downstream mTOR-related readouts, whereas Rapalink-1 reduced several of these signaling-associated responses.

In summary, Rapalink-1 attenuated key components of the SC-induced vascular stress response in vitro. These findings support further investigation of mTOR-related signaling as a regulatory pathway in smoking-related vascular injury and vascular aging.

List of Abbreviations

8-OHDG	8-hydroxy-2′-deoxyguanosine
AKT	protein kinase B
BSA	bovine serum albumin
PTGS2	cyclooxygenase-2
DCFH-DA	2′,7′-dichlorofluorescein diacetate
DDR	DNA damage response
ECM	extracellular matrix
ERK	extracellular signal-regulated kinase (ERK1/2)
GAPDH	glyceraldehyde-3-phosphate dehydrogenase
HMOX1	heme oxygenase-1
HUVECs	human umbilical vein endothelial cells
ICAM-1	intercellular adhesion molecule-1
Lamin B1	nuclear lamin B1
IF	immunofluorescence
NOS2	inducible nitric oxide synthase
MAPK	mitogen-activated protein kinase
SOD2	manganese superoxide dismutase
MMP(s)	matrix metalloproteinase(s)
mTOR	mechanistic target of rapamycin
MTT	3-(4,5-dimethylthiazol-2-yl)-2,5-diphenyltetrazolium bromide
NF-κB	nuclear factor kappa-light-chain-enhancer of activated B cells
NOX4	NADPH oxidase 4
NFE2L2	nuclear factor erythroid 2–related factor 2
p21	cyclin-dependent kinase inhibitor 1
p38	p38 mitogen-activated protein kinase (MAPK14)

p65	nuclear factor kappa-light-chain-enhancer of activated B cells p65 (RelA)
RIPA	radioimmunoprecipitation assay (buffer)
ROS	reactive oxygen species
RT	room temperature
SA-β-gal	senescence-associated β-galactosidase
SASP	senescence-associated secretory phenotype
SC	smoke condensate (tobacco smoke condensate)
SMCs	smooth muscle cells (vascular)
S6	ribosomal protein S6
TBST	Tris-buffered saline with Tween-20
TIMP(s)	tissue inhibitor(s) of metalloproteinases
TNF-α	tumor necrosis factor-alpha
γ-H2AX	phosphorylated H2A histone family member X (Ser139)
VCAM1	vascular cell adhesion molecule 1

Table of Contents

1. Introduction

1.1. Background and Rationale

Smoking is a leading preventable risk factor for cardiovascular and cerebrovascular disease. It promotes endothelial dysfunction, oxidative stress, inflammation, platelet activation, thrombosis, and acceleration of atherosclerosis [1–4]. Smoking is also strongly associated with cerebrovascular pathology, including ischemic stroke and aneurysm-related vascular injury [5–7]. These clinical associations indicate that tobacco-derived compounds affect the vessel wall, but the cellular mechanisms underlying smoke-induced vascular damage remain incompletely defined.

Vascular homeostasis depends on the coordinated function of endothelial cells and vascular smooth muscle cells. Endothelial cells regulate barrier function, vascular tone, leukocyte adhesion, and anticoagulant properties [8–10]. Smooth muscle cells contribute to contractility, extracellular matrix production, and adaptation to injury [11,12]. Damage to either cell type can promote chronic inflammation, matrix remodeling, and structural weakening of the vessel wall.

Cellular senescence may connect persistent smoke exposure to long-term vascular dysfunction. Senescent cells show stable cell-cycle arrest together with nuclear changes, DNA damage signaling, metabolic alterations, and inflammatory secretory activity [13–15]. In the vascular wall, senescent endothelial cells and smooth muscle cells have been linked to vascular aging, endothelial dysfunction, atherosclerosis, and vessel wall degeneration [16–18]. Smoke-induced senescence may therefore contribute to accelerated vascular aging.

Oxidative stress and DNA damage are central drivers of stress-induced senescence. Cigarette smoke contains reactive species that disturb redox balance and damage proteins, lipids, and DNA [19,20]. Persistent oxidative injury can activate DNA damage responses and stress-related signaling pathways, thereby promoting premature senescence and inflammatory remodeling. Smoke condensate provides a controlled in vitro model to study these effects in vascular cells.

In this thesis, human umbilical vein endothelial cells and vascular smooth muscle cells were exposed to smoke condensate. The study examined oxidative stress, DNA damage, senescence markers, the senescence-associated secretory phenotype, extracellular

matrix remodeling, and NF-κB-, MAPK-, and mTOR-related signaling. Rapalink-1, a dual mTORC1/2 inhibitor, was then assessed to determine whether it attenuates these smoke-induced responses.

1.2. Tobacco Smoke Condensate as an Experimental Model of Vascular Injury

Tobacco smoke contains a wide range of reactive and chemically active compounds, including reactive oxygen species, aldehydes, polycyclic aromatic hydrocarbons, nitrosamines, and particulate matter [21]. These components can damage the vessel wall through oxidative injury, inflammatory signaling, endothelial dysfunction, pro-thrombotic changes, and ECM remodeling. Experimental models that capture defined aspects of smoke exposure are therefore useful for studying how tobacco-derived toxicants affect vascular cells.

Tobacco smoke condensate (SC) and cigarette smoke extract are two commonly used in vitro approaches for this purpose. Neither system fully replicates chronic smoking in vivo, but both allow reproducible exposure of cultured cells to tobacco-derived toxicants. In endothelial cells, smoke-derived preparations have been shown to impair cell function, increase oxidative stress, alter inflammatory responses, and disturb protective signaling pathways [22–25]. These observations support the use of SC as a relevant in vitro model for studying vascular stress responses.

The limitations of this model should also be considered. SC exposure in cultured cells does not include systemic metabolism, immune cell recruitment, platelet activation, hemodynamic forces, or long-term tissue adaptation. Nevertheless, endothelial dysfunction is an early hallmark of vascular disease, and cultured endothelial cell systems remain useful for studying mechanisms related to inflammation, thrombosis, and atherosclerosis [26–30]. SC exposure therefore provides a defined experimental setting for examining early vascular injury mechanisms before evaluation in more complex models.

HUVECs and SMCs have distinct roles in vascular homeostasis and may respond differently to smoke-derived stress. Endothelial injury can promote leukocyte adhesion, barrier dysfunction, loss of antithrombotic properties, and inflammatory activation. In contrast, SMC injury may affect phenotypic stability and ECM maintenance. Both cell types are relevant to chronic vascular disease, including atherosclerosis and vessel

remodeling [31–35]. Studying both cell types therefore provides complementary perspectives on smoke-induced vascular injury.

In this thesis, SC was used to induce stress responses in HUVECs and SMCs. Oxidative stress, DNA damage, senescence-associated changes, inflammatory mediator expression, ECM-related alterations, and intracellular signaling were assessed. Rapalink-1, a dual mTORC1/2 inhibitor, was then tested to determine whether it attenuates SC-induced vascular cell injury.

1.3. Oxidative and Genotoxic Stress in Smoke-Exposed Vascular Cells

Oxidative and genotoxic stress are major mechanisms through which tobacco-derived compounds damage vascular cells. Cigarette smoke contains reactive species and chemically active substances that can disturb redox homeostasis directly or promote secondary oxidative reactions after cellular uptake [19–21]. Under physiological conditions, ROS contribute to intracellular signaling and vascular regulation. When ROS production becomes excessive or sustained, antioxidant defenses may be overwhelmed, leading to damage of proteins, lipids, and nucleic acids [36,37]. In vascular tissue, this imbalance contributes to endothelial dysfunction, impaired nitric oxide signaling, inflammatory activation, and phenotypic changes in SMCs [26,31–39].

In smoke-exposed vascular cells, oxidative stress is closely linked to DNA damage and premature senescence. ROS can induce oxidative base modifications, DNA strand breaks, and activation of the DNA damage response (DDR) [40,41]. If these lesions persist or are insufficiently repaired, checkpoint activation may promote stable growth arrest and senescence-associated remodeling [42,43]. Therefore, smoke-induced vascular senescence should be assessed using a panel of complementary markers rather than a single readout. In the present study, oxidative stress readouts, DNA damage markers, cell-cycle regulators, nuclear structural changes, and senescence-associated enzymatic activity were evaluated to determine whether SC induces an oxidative, genotoxic, and senescence-associated phenotype in vascular cells [44,45].

1.3.1. Senescence-Associated β-Galactosidase Activity

Senescence-associated β-galactosidase (SA-β-gal) activity is widely used to identify senescent cells in culture [46–48]. It reflects increased lysosomal β-galactosidase

activity under specific staining conditions and enables visualization and quantification of senescent cells in vitro [46]. In vascular cell models, positive SA-β-gal staining provides an initial indication that a stressor has induced a senescence-associated phenotype.

However, SA-β-gal activity is not specific for senescence and should not be interpreted as a standalone marker [49]. Staining intensity can be influenced by cell type, culture conditions, cell density, and the type of stress applied. Some senescent cells may show weak staining, whereas non-senescent cells can become positive under certain conditions. Therefore, SA-β-gal staining is most informative when assessed together with additional markers, such as p21 expression, Lamin B1 loss, and DNA damage readouts. In smoke-induced vascular injury, increased SA-β-gal activity supports the presence of a senescence-associated phenotype but does not by itself prove senescence.

1.3.2. Lamin B1 Expression

Lamin B1 is a structural protein of the nuclear lamina and contributes to nuclear architecture, chromatin organization, and genome stability. Loss of Lamin B1 is a well-described feature of senescent cells and is frequently used as a marker of senescence-associated nuclear remodeling [50,51]. Unlike SA-β-gal activity, which reflects lysosomal changes, reduced Lamin B1 expression provides information on structural alterations of the nucleus during senescence.

During stable senescence-associated growth arrest, Lamin B1 reduction is thought to accompany changes in nuclear integrity and chromatin organization [44,45,50,51]. In vascular cells exposed to smoke-derived stressors, Lamin B1 loss may therefore indicate that the cellular response extends beyond transient oxidative injury and involves senescence-associated nuclear remodeling. Assessment of Lamin B1 together with SA-β-gal staining, p21 expression, and DNA damage markers provides a more robust basis for interpreting senescence-related changes.

1.3.3. p21 Expression

p21, also known as cyclin-dependent kinase inhibitor 1A, is an important regulator of cell-cycle arrest and cellular senescence [52,53]. It can be induced by DNA damage, oxidative stress, p53 activation, and other stress-related signals. Through inhibition of cyclin-dependent kinases, p21 limits cell-cycle progression and contributes to the establishment of a growth-arrested state [52–54].

In stress-induced senescence, sustained p21 expression is commonly used as molecular evidence of a senescence-associated growth-arrest program. In vascular cells exposed to SC, increased p21 expression may link oxidative injury and DDR activation to senescence establishment. However, p21 can also increase during acute stress responses. Therefore, p21 levels are most informative when interpreted together with other senescence-associated changes, including Lamin B1 loss, SA-β-gal activity, and accumulation of DNA damage markers.

1.3.4. Reactive Oxygen Species and DCFH-DA

ROS play a central role in smoke-induced cellular injury. Tobacco smoke contains reactive compounds and can also activate endogenous ROS-generating systems, thereby amplifying oxidative stress after exposure [19–23,36,37]. In vascular cells, excessive ROS production can impair endothelial function, reduce nitric oxide bioavailability, activate inflammatory signaling, and promote phenotypic remodeling in SMCs [31–39]. These effects provide a mechanistic basis for the link between smoke exposure, vascular dysfunction, and premature vascular aging.

The fluorescent probe 2′,7′-dichlorodihydrofluorescein diacetate (DCFH-DA) is commonly used to assess the overall intracellular oxidative state in cultured cells [55]. After cellular uptake and oxidation, DCFH-DA generates a fluorescent signal that reflects oxidation-sensitive intracellular changes. However, this method does not identify the specific ROS species involved or define the subcellular source of the signal [55–57]. DCFH-DA-based results should therefore be interpreted as a general oxidative stress readout rather than evidence for a particular ROS type. In smoke-induced vascular injury models, this readout is most informative when assessed together with downstream markers of oxidative damage, DNA injury, and senescence-associated changes.

1.3.5. γ-H2AX and 8-OHDG

DNA damage is an important downstream consequence of persistent oxidative stress and contributes to stress-induced senescence. Oxidative injury can cause base modifications, DNA strand breaks, and activation of the DNA damage response [40,41]. γ-H2AX, the phosphorylated form of histone H2AX, is widely used as a readout of DNA double-strand break signaling and DDR activation [58,59]. Increased γ-H2AX staining therefore indicates activation of genotoxic stress signaling rather than nonspecific cellular damage alone.

8-hydroxy-2′-deoxyguanosine (8-OHDG) reflects oxidative modification of DNA bases, particularly guanine [60–62]. Whereas γ-H2AX mainly indicates DDR activation, 8-OHDG provides information on oxidative base damage. These two markers therefore provide complementary information in smoke-exposed vascular cells. Their combined assessment is relevant because oxidative stress and genotoxic injury are closely linked and may together contribute to the development of senescence-associated phenotypes.

1.3.6. Senescence-Associated Secretory Phenotype

Cellular senescence involves more than growth arrest. Senescent cells undergo phenotypic remodeling and can influence their local environment through the secretion of inflammatory cytokines, chemokines, adhesion molecules, growth factors, and proteases. This secretory program is referred to as the senescence-associated secretory phenotype (SASP) [63–66]. Through autocrine and paracrine signaling, the SASP can reinforce senescence and affect neighboring cells, thereby linking cellular senescence to tissue inflammation and remodeling.

In vascular aging and smoke-related vascular injury, the SASP is relevant because endothelial cells and SMCs regulate vascular inflammation, leukocyte recruitment, and ECM homeostasis [26–35,67]. Senescent vascular cells may increase the expression of inflammatory mediators such as TNF-α and adhesion molecules such as ICAM-1 and VCAM-1. They may also alter matrix-remodeling enzymes and their regulators, including matrix metalloproteinases (MMPs) and tissue inhibitors of metalloproteinases (TIMPs) [68–70]. These changes can disturb ECM turnover and may contribute to vessel wall dysfunction, stiffness, and structural damage.

The present study examined SASP- and ECM-related changes in SC-exposed vascular cells. In HUVECs, SC increased the expression of several inflammatory and matrix-related transcripts, including TNF-α, ICAM1, MMP1, MMP10, and TIMP3, whereas PTGS2 remained elevated despite Rapalink-1 treatment. In SMCs, SC was associated with marked ECM-related alterations, including reduced expression of ELN, COL1A1, and EFEMP1. Protein-level analyses also showed increased MMP-2 and VCAM-1 expression under smoke stress. These findings indicate that SC induces not only intracellular stress and senescence-associated marker changes, but also inflammatory and matrix-remodeling responses relevant to vascular pathology.

Rapalink-1 attenuated several of these SASP- and ECM-related responses. Co-treatment reduced the SC-induced upregulation of selected inflammatory and

remodeling genes and partially normalized structural ECM-associated transcripts. These observations suggest that Rapalink-1 may affect downstream secretory and remodeling programs in addition to reducing oxidative stress and DNA damage. Because the SASP can sustain chronic inflammation and tissue dysfunction, its attenuation may be relevant for limiting smoke-related vascular injury.

Taken together, oxidative stress, DNA damage, senescence-associated marker changes, SASP activation, and ECM remodeling appear to be linked components of the SC-induced vascular stress response. Assessing these processes together provides a more complete basis for understanding how SC promotes vascular cell dysfunction and how mTORC1/2 inhibition with Rapalink-1 may modulate this response.

1.4. NF-κB, MAPK, and mTOR-Related Signaling Networks

Oxidative stress, DNA damage, cellular senescence, inflammation, and ECM remodeling are regulated by interacting signaling pathways rather than by isolated molecular events. In smoke-exposed vascular cells, early oxidative and genotoxic injury can lead to sustained changes in gene transcription, protein phosphorylation, cell-cycle regulation, inflammatory mediator expression, and matrix remodeling. NF-κB, MAPK, and mTOR-related signaling are among the pathways most relevant to these processes [71–76].

NF-κB is a key transcriptional regulator of inflammatory and stress-responsive genes. Under basal conditions, NF-κB proteins are retained in the cytoplasm through interaction with inhibitory IκB proteins. In response to pro-inflammatory cytokines, oxidative stress, DNA damage, or other stressors, this inhibitory system can be disrupted, allowing NF-κB to translocate to the nucleus and regulate target-gene transcription [71,72]. These targets include cytokines, chemokines, adhesion molecules, anti-apoptotic proteins, and mediators involved in tissue remodeling. In vascular cells, NF-κB activation is closely linked to endothelial activation, leukocyte adhesion, inflammatory amplification, and chronic vascular injury [73,74].

NF-κB is also relevant to senescence biology. In senescent cells, NF-κB contributes to SASP regulation [75,76]. Persistent NF-κB activity can maintain the expression of pro-inflammatory mediators and support a local environment in which senescent cells influence neighboring cells. In smoke-exposed vascular cells, this pathway may link oxidative stress and DNA damage to SASP-related gene expression, endothelial

activation, and ECM remodeling. For this reason, p65 and phosphorylated p65 were assessed as readouts of NF-κB-related inflammatory signaling.

MAPK signaling provides another link between cellular stress and adaptive or maladaptive cellular responses. The MAPK family includes several conserved kinase cascades, among which ERK, p38 MAPK, and JNK are the best characterized [77,78]. These pathways are activated through sequential phosphorylation and regulate transcription factors, kinases, and other downstream effectors involved in proliferation, differentiation, survival, apoptosis, inflammation, and stress responses [77–80]. In vascular cells, MAPK activation can occur in response to oxidative stress, inflammatory mediators, growth factors, mechanical forces, and toxic environmental stimuli.

p38 MAPK and ERK-related signaling are particularly relevant in the context of senescence. p38 MAPK has been linked to the expression of senescence-associated inflammatory mediators and can regulate SASP-related responses independently of classical DDR signaling [81,82]. MAPK pathways can also influence senescence-associated traits by connecting stress signals to cell-cycle arrest, inflammatory gene programs, and post-transcriptional regulation [83]. In addition, crosstalk between MAPK signaling and NF-κB activity may amplify inflammatory responses, as p38-related mechanisms can modulate NF-κB activity under stress conditions [84]. In the present study, phosphorylation of p38 and ERK was examined to assess stress-activated kinase signaling after SC exposure and Rapalink-1 treatment.

mTOR-related signaling represents an additional regulatory layer in smoke-exposed vascular cells. mTOR is a central kinase that integrates nutrient availability, growth factor signaling, energy status, protein synthesis, autophagy, metabolism, and cellular stress adaptation [85–87]. It functions mainly through two multiprotein complexes, mTORC1 and mTORC2, which differ in upstream regulation, downstream targets, and biological functions [85–91]. mTORC1 is closely linked to protein synthesis, ribosome biogenesis, nutrient sensing, and autophagy regulation, whereas mTORC2 contributes to AKT signaling, cytoskeletal organization, and survival-associated pathways.

In aging and senescence biology, mTOR signaling is relevant because it can influence metabolic remodeling, proteostasis, autophagy, inflammatory output, and the persistence of senescence-associated phenotypes [85–89,92]. Experimental studies have shown that pharmacological mTOR inhibition can affect aging-associated processes, supporting the concept that mTOR is a modifiable regulator of cellular aging

[92]. In vascular cells exposed to toxic stress, mTOR-related signaling may therefore contribute not only to cell survival and metabolic adaptation, but also to inflammatory secretion, senescence-associated remodeling, and ECM-related responses.

Experimental work also suggests that cigarette smoke can engage mTOR-associated stress pathways in disease models [93]. This is relevant to the present study because SC induced a vascular stress phenotype involving oxidative stress, DNA damage, senescence-associated marker changes, inflammatory mediator expression, and ECM remodeling. These findings support the view that NF-κB, MAPK, and mTOR-related pathways may jointly contribute to smoke-induced vascular cell dysfunction.

1.5. Rapalink-1 and Its Potential Relevance in Vascular Disease

Rapalink-1 is a dual mTORC1/2 inhibitor developed to overcome several limitations of earlier mTOR-targeted compounds [94]. Classical rapamycin and its analogues have provided important insight into mTOR biology, but their inhibitory effects are incomplete and context-dependent. Some mTORC1 outputs are relatively resistant to short-term rapamycin treatment, and prolonged exposure can also affect mTORC2 assembly and AKT signaling [95–98]. These properties are relevant when interpreting vascular stress models, because smoke-induced injury involves oxidative stress, inflammation, metabolic adaptation, senescence-associated remodeling, and ECM changes.

ATP-competitive mTOR kinase inhibitors were developed to target rapamycin-resistant mTOR outputs and to inhibit both mTORC1- and mTORC2-related signaling [97,98]. These compounds showed that mTOR regulates a broader range of downstream processes than those captured by rapamycin-sensitive readouts alone. mTOR activity influences protein synthesis, translational control, metabolism, autophagy, AKT-related signaling, and cell growth adaptation [85–91,99,100]. These processes are relevant to senescence because senescent cells remain metabolically active and can maintain inflammatory secretory programs despite stable proliferative arrest.

Rapalink-1 combines rapamycin-binding and kinase-inhibitory properties and was designed to achieve more durable mTOR inhibition [94]. This pharmacological profile is useful in experimental settings in which both mTORC1- and mTORC2-related outputs may contribute to stress responses. In the present study, this was relevant because SC altered downstream mTOR-related readouts, including S6- and AKT-

associated phosphorylation signals. These readouts provide information on pathway output, although they do not fully define the activity state of mTORC1 or mTORC2.

The use of Rapalink-1 in smoke-exposed vascular cells is further supported by the role of mTOR in aging and stress biology. mTOR signaling has been linked to aging-associated phenotypes, immune function, protein synthesis, autophagy regulation, and metabolic remodeling [85–89,92,101]. Experimental studies have also shown that mTOR inhibition can influence senescence-associated phenotypes and delay aspects of cellular aging [92,102,103]. These findings support the view that mTOR-related signaling may contribute to the maintenance or amplification of stress-induced senescence.

In vascular cells, the relevance of Rapalink-1 is not limited to direct changes in mTOR downstream phosphorylation. SC induces oxidative injury, DNA damage, inflammatory signaling, SASP-related mediator expression, and ECM remodeling. Because these processes occur in parallel and may influence one another, mTORC1/2 inhibition may affect several phenotypic outcomes. This does not imply that Rapalink-1 acts as a direct antioxidant or that all observed effects are exclusively mTOR-dependent. Rather, Rapalink-1 should be interpreted as a pharmacological tool to examine how mTOR-related signaling contributes to SC-induced vascular cell stress.

Previous work from our group showed that Rapalink-1 attenuated ethanol-induced endothelial senescence, providing a rationale for testing this compound in an additional vascular stress model [104]. The present thesis extends this work to SC-induced vascular injury and includes both HUVECs and SMCs. This cellular approach is relevant because smoking-related vascular disease affects multiple vascular compartments, and SMC dysfunction may be particularly important for ECM remodeling and vessel wall integrity.

In the present study, Rapalink-1 attenuated several SC-induced responses, including oxidative stress readouts, DNA damage markers, senescence-associated changes, SASP-related transcriptional alterations, ECM-related changes, and phosphorylation-associated signaling responses. These findings support the interpretation that Rapalink-1 affects multiple components of the smoke-induced vascular stress response. However, the results should be interpreted within the limitations of the in vitro model. Further studies using pathway-specific rescue experiments, genetic approaches, and disease-relevant in vivo models will be required to define the relative contribution of mTORC1,

mTORC2, and downstream signaling nodes to the effects observed here.

1.6. Aims of the Thesis

The present thesis had three main aims. First, it aimed to determine whether SC induces vascular cell injury in HUVECs and SMCs, with a focus on oxidative stress, DNA damage, cellular senescence, inflammatory activation, and ECM remodeling.

Second, it aimed to assess whether Rapalink-1 attenuates SC-induced injury responses. For this purpose, several complementary readouts were evaluated, including ROS-associated fluorescence, DNA damage markers, SA-β-gal activity, Lamin B1 expression, p21 expression, SASP-related gene expression, ECM-related transcripts, and selected protein-level markers.

Third, the thesis examined whether these cellular responses are associated with changes in NF-κB-, MAPK-, and mTOR-related signaling. By integrating phenotypic, transcriptional, and protein-level data, the study assessed whether dual mTORC1/2 inhibition with Rapalink-1 affects key components of the SC-induced vascular stress response.

1.7. Ethics Statement

The experimental work was performed using commercially obtained human vascular cell models and did not involve the direct recruitment of human participants or the collection of new patient-derived samples. All experiments were conducted in accordance with the institutional requirements of the Medical Faculty and University Hospital Düsseldorf. Where applicable, the use of human cell material followed the supplier's documentation and the relevant institutional regulations.

2. Published Original Article

The following published original article forms the basis of this publication-based dissertation:

You, J., Liu, H., Khan, D., Muhereza, R., Faust, K., & Muhammad, S. (2026).

Smoke Condensate-Induced Vascular Senescence and SASP Are Attenuated by Dual mTORC1/2 Inhibition with Rapalink-1.

International Journal of Molecular Sciences, 27(8), 3636.

https://doi.org/10.3390/ijms27083636

The published article is reproduced on the following pages.

International Journal of
Molecular Sciences

MDPI

Article

Smoke Condensate-Induced Vascular Senescence and SASP Are Attenuated by Dual mTORC1/2 Inhibition with Rapalink-1

Jinliang You, Hongjun Liu, Dilaware Khan, Robert Muhereza, Katharina Faust and Sajjad Muhammad *

Department of Neurosurgery, Medical Faculty, University Hospital Düsseldorf, Heinrich-Heine-Universität Düsseldorf, Moorenstr. 5, 40225 Düsseldorf, Germany; jinliangyou8@gmail.com (J.Y.); hongjunliu303@gmail.com (H.L.); dilaware00@yahoo.com (D.K.); robertlana0@gmail.com (R.M.); katharinaangela.faust@med.uni-duesseldorf.de (K.F.)

* Correspondence: sajjad.muhammad@med.uni-duesseldorf.de; Tel.: +49-211-81-07823

Abstract

Cigarette smoking contributes to vascular aging through oxidative stress, inflammation, and extracellular matrix (ECM) remodeling. Cellular senescence has been recognized as an important mechanism linking tobacco exposure to vascular dysfunction, but effective pharmacological strategies targeting this process remain scarce. In this study, we examined whether Rapalink-1, a dual inhibitor of mechanistic target of rapamycin complex 1 and complex 2 (mTORC1 and mTORC2), modulates smoke condensate (SC)-induced senescence in vascular cells. Human umbilical vein endothelial cells (HUVECs) and vascular smooth muscle cells (SMCs) were exposed to SC with or without Rapalink-1. SC increased intracellular reactive oxygen species, induced DNA damage, and promoted senescence-associated changes, including increased senescence-associated β-galactosidase (SA-β-gal) activity, reduced Lamin B1, and elevated p21 expression. These effects were accompanied by increased expression of inflammatory and matrix-remodeling genes associated with the senescence-associated secretory phenotype (SASP). Rapalink-1 co-treatment reduced oxidative stress and DNA damage, attenuated senescence markers, and partially normalized SASP-related and ECM-associated gene expression. Mechanistically, SC activated nuclear factor kappa B (NF-κB) and mitogen-activated protein kinase (MAPK) signaling and increased downstream mTOR pathway activity, whereas Rapalink-1 dampened these signaling responses. Together, these findings indicate that dual mTORC1/2 inhibition by Rapalink-1 mitigates smoke condensate-induced senescence and inflammatory responses in vascular cells.

Keywords: rapalink-1; mTOR; vascular senescence; SASP

Academic Editor: David Della-Morte

Received: 6 March 2026
Revised: 10 April 2026
Accepted: 16 April 2026
Published: 19 April 2026

1. Introduction

Tobacco smoking remains one of the leading preventable causes of cardiovascular and cerebrovascular morbidity and mortality worldwide, strongly predisposing individuals to atherosclerosis, intracranial aneurysms, and stroke [1–4]. Beyond its systemic toxicity, cigarette smoke exerts profound deleterious effects on the vascular wall by promoting oxidative stress, chronic inflammation, and extracellular matrix (ECM) remodeling, thereby accelerating vascular aging and structural degeneration [5–8]. Epidemiological evidence consistently demonstrates that smokers exhibit an increased incidence of vascular disease and worse clinical outcomes compared with non-smokers [9–11]. However, the intracellular signaling networks that mechanistically link tobacco exposure to vascular degeneration remain incompletely understood.

Accumulating evidence suggests that cellular senescence is an important mechanism linking tobacco smoke exposure to vascular aging [12,13]. Persistent oxidative and genotoxic stress induced by cigarette smoke drives premature senescence in both endothelial cells and vascular smooth muscle cells. Senescent vascular cells display characteristic molecular features, including increased senescence-associated β-galactosidase (SA-β-gal) activity, depletion of nuclear Lamin B1, accumulation of DNA damage markers such as phosphorylated H2A histone family member X (γ-H2AX) and 8-hydroxy-2′-deoxyguanosine (8-OHDG), and sustained cell-cycle arrest [14–16]. Importantly, senescent cells acquire a senescence-associated secretory phenotype (SASP), marked by excessive production of pro-inflammatory cytokines, chemokines, and matrix-degrading enzymes, which collectively amplify local inflammation and ECM disruption. Through these processes, cellular senescence contributes to vascular wall weakening, maladaptive remodeling, and disease progression in conditions such as aneurysm formation, atherogenesis, and vascular stiffening [17–20]. Despite its pathogenic relevance, effective pharmacological strategies to suppress smoke-induced vascular senescence remain limited.

To dissect these mechanisms under controlled conditions, tobacco smoke condensate (SC)—the particulate phase of cigarette smoke—is widely employed as an in vitro model of smoke-induced vascular injury [21–23]. SC exposure robustly induces reactive oxygen species (ROS) accumulation, mitochondrial dysfunction, and DNA damage in endothelial and smooth muscle cells, ultimately triggering premature senescence [12,22,24]. These stress responses converge on key signaling pathways, including nuclear factor kappa B (NF-κB) and mitogen-activated protein kinase (MAPK), which orchestrate inflammatory and stress-adaptive transcriptional programs, as well as the mTOR pathway, a central regulator of cellular metabolism, growth, and aging. Persistent activation of these pathways reinforces oxidative and inflammatory signaling, promotes SASP activation, and drives maladaptive ECM remodeling—hallmarks of smoking-associated vascular degeneration. However, therapeutic approaches targeting individual downstream consequences, such as antioxidants or anti-inflammatory agents, have shown limited efficacy, underscoring the need for interventions that modulate upstream signaling nodes governing senescence and stress integration.

The mechanistic target of rapamycin (mTOR) pathway has emerged as a master regulator linking nutrient sensing, stress responses, and cellular aging. Chronic mTOR activation accelerates oxidative stress, inflammatory signaling, and senescence, whereas mTOR inhibition extends lifespan and alleviates age-related pathologies across multiple species [25–28]. Rapalink-1 is a third-generation dual mTORC1/2 inhibitor that overcomes limitations of earlier mTOR inhibitors and exhibits enhanced potency and durability [29,30]. Beyond its established roles in cancer and metabolic disease, recent studies demonstrate that Rapalink-1 confers cytoprotective effects by coordinately suppressing NF-κB, MAPK, and mTOR signaling, thereby attenuating stress-induced cellular dysfunction [31]. Notably, dual mTORC1/2 inhibition also impacts protein kinase B (AKT) signaling, a critical stress-adaptive pathway implicated in cellular survival and homeostasis, suggesting that Rapalink-1 may fine-tune signaling networks rather than simply abrogate them.

Based on these considerations, we hypothesized that Rapalink-1 protects vascular endothelial and smooth muscle cells from tobacco smoke condensate-induced oxidative stress, DNA damage, and premature senescence by reprogramming interconnected inflammatory and metabolic signaling pathways. By integrating cellular, molecular, and transcriptional analyses, the present study aimed to determine whether dual mTORC1/2 inhibition by Rapalink-1 mitigates SC-induced vascular injury through coordinated modulation of NF-κB/MAPK signaling, mTOR signaling to ribosomal protein S6 (S6) output, and stress-adaptive AKT activation. This work provides mechanistic insight into how targeting

senescence-associated signaling networks may offer a promising therapeutic strategy to counteract smoking-related vascular aging and degeneration.

2. Results

2.1. Rapalink-1 Alleviates SC-Induced Oxidative Stress and Restores Cell Viability in HUVECs and SMCs

To determine whether SC induces oxidative stress and whether Rapalink-1 can counteract this response, intracellular ROS levels were first evaluated using 2′,7′-dichlorodihydrofluorescein diacetate (DCFH-DA) staining.

In HUVECs, SC markedly increased DCFH-DA-derived fluorescent signals, indicating elevated intracellular oxidative stress, whereas Rapalink-1 alone did not appreciably affect basal staining. Notably, co-treatment with Rapalink-1 significantly reduced the SC-induced increase in DCFH-DA-positive cells (Percentage of positive cells: Control = 0.90 ± 1.56%; SC = 62.93 ± 1.58%; Rapalink-1 = 0.49 ± 0.43%; SC + Rapalink-1 = 5.20 ± 2.30%; $p < 0.0001$; Figure 1A,B). In SMCs, a similar oxidative response was observed following SC exposure (Supplementary Figure S1).

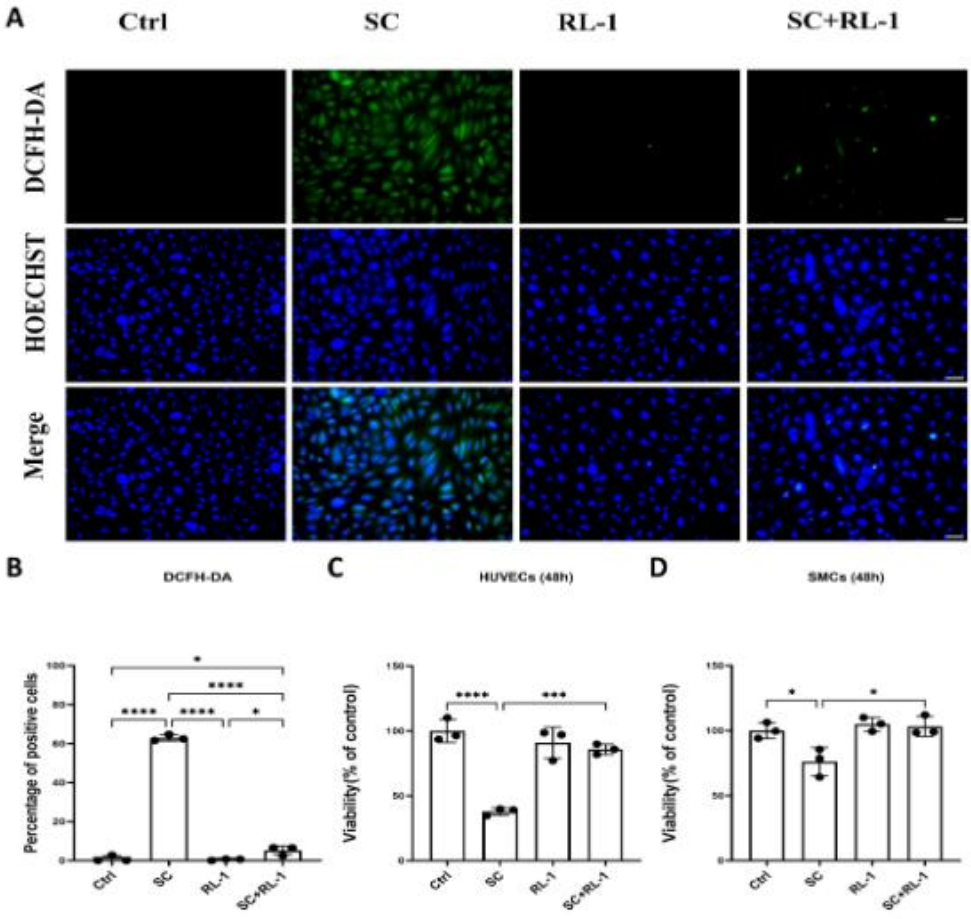

Figure 1. (**A**) Representative fluorescence images of DCFH-DA staining (green) with Hoechst nuclear counterstaining (blue) in HUVECs after 2 h treatment under four conditions: Control (Ctrl), SC, Rapalink-1 (RL-1), and SC + RL-1. (**B**) Quantification of DCFH-positive cells (%) in HUVECs. (**C**,**D**) Cell metabolic viability measured by MTT assay in HUVECs and SMCs at 48 h. Scale bar = 50 µm, Data are presented as mean ± SD ($n = 3$). Statistical significance was determined by one-way ANOVA with Tukey's multiple comparisons test. Significance is indicated as: * $p < 0.05$, *** $p < 0.001$, **** $p < 0.0001$.

Consistent with these findings, SC stimulation induced a coordinated oxidative stress-related transcriptional response in both HUVECs and SMCs, including NOX4 and NOS2, as well as activation of antioxidant defense pathways such as HMOX1, SOD2, and the redox-responsive transcription factor NFE2L2. Rapalink-1 alone also caused modest changes in a subset of transcripts in HUVECs, although these were generally smaller than the SC-induced responses. Importantly, Rapalink-1 co-treatment selectively attenuated parts of this stress-responsive gene program, with the strongest suppression observed for NOS2, SOD2, and NFE2L2, whereas in HUVECs, HMOX1 remained elevated despite Rapalink-1 treatment (Tables 1 and 2).

Table 1. Quantification of relative mRNA expression in HUVECs (*p* values: overall one-way ANOVA across the four groups; Tukey post hoc for pairwise comparisons).

Gene	Control	SC	Rapalink-1	SC + Rapalink-1	*p*-Value
NOX4	1.06 ± 0.39	2.80 ± 0.30	0.88 ± 0.20	2.54 ± 0.81	0.0021
NOS2	1.08 ± 0.48	15.69 ± 8.49	6.81 ± 5.73	0.70 ± 0.04	0.0231
HMOX1	1.12 ± 0.67	20.07 ± 4.40	0.85 ± 0.25	25.01 ± 6.88	0.0001
SOD2	1.05 ± 0.41	7.35 ± 3.10	3.16 ± 1.21	1.18 ± 0.29	0.0058
NFE2L2	1.07 ± 0.52	3.78 ± 1.92	1.63 ± 0.94	0.73 ± 0.21	0.0371
MMP1	1.00 ± 0.14	23.13 ± 5.46	0.65 ± 0.07	17.02 ± 3.52	<0.0001
MMP10	1.07 ± 0.49	5.46 ± 1.31	0.78 ± 0.26	3.09 ± 0.70	0.0003
MMP11	1.02 ± 0.21	1.21 ± 0.11	0.95 ± 0.04	0.89 ± 0.03	0.0464
TIMP3	1.02 ± 0.25	2.75 ± 1.15	1.14 ± 0.45	0.66 ± 0.32	0.0179
TIMP4	1.09 ± 0.49	3.22 ± 1.21	2.11 ± 1.39	0.78 ± 0.22	0.0522
TNF-α	1.01 ± 0.23	2.85 ± 0.28	1.62 ± 0.25	1.10 ± 0.33	0.0001
PTGS2	1.21 ± 0.74	5.20 ± 3.52	1.73 ± 0.19	7.58 ± 3.44	0.0423
ICAM1	1.01 ± 0.16	6.44 ± 3.13	2.49 ± 1.15	0.93 ± 0.17	0.0118

Table 2. Quantification of relative mRNA expression in SMCs (*p* values: overall one-way ANOVA across the four groups; Tukey post hoc for pairwise comparisons).

Gene	Control	SC	Rapalink-1	SC + Rapalink-1	*p*-Value
NOX4	1.06 ± 0.42	1.74 ± 0.28	1.28 ± 0.36	1.09 ± 0.09	0.0931
NOS2	2.32 ± 2.47	15.15 ± 2.43	5.25 ± 3.00	5.80 ± 2.27	0.0014
HMOX1	1.13 ± 0.68	14.19 ± 5.70	1.28 ± 0.24	7.37 ± 1.85	0.0021
SOD2	1.07 ± 0.45	2.90 ± 1.00	1.71 ± 0.18	1.54 ± 0.68	0.0446
NFE2L2	1.08 ± 0.46	3.91 ± 1.39	1.72 ± 0.15	1.84 ± 0.92	0.0195
MMP1	1.08 ± 0.50	35.01 ± 11.49	1.38 ± 0.14	1.31 ± 0.55	0.0002
MMP10	1.59 ± 1.80	5.42 ± 1.97	2.62 ± 0.36	1.82 ± 0.64	0.0329
MMP11	1.09 ± 0.50	2.28 ± 0.61	1.57 ± 0.17	1.67 ± 0.53	0.0938
TIMP3	1.02 ± 0.27	5.12 ± 2.03	1.93 ± 0.53	1.15 ± 0.07	0.0046
TIMP4	1.01 ± 0.16	5.47 ± 2.56	2.16 ± 0.24	1.06 ± 0.55	0.0098
TNF-α	1.03 ± 0.32	3.97 ± 1.58	1.55 ± 1.05	1.52 ± 0.19	0.0227
PTGS2	1.09 ± 0.59	4.96 ± 1.08	1.71 ± 0.35	2.05 ± 0.83	0.0012
ICAM1	1.06 ± 0.45	2.71 ± 0.67	0.95 ± 0.23	1.30 ± 0.34	0.0050
ELN	1.02 ± 0.28	0.16 ± 0.03	1.21 ± 0.22	0.82 ± 0.30	0.0026
COL1A1	1.01 ± 0.19	0.21 ± 0.02	1.34 ± 0.13	1.07 ± 0.16	<0.0001
EFEMP1	1.02 ± 0.20	0.49 ± 0.05	1.46 ± 0.20	0.95 ± 0.09	0.0003

We next examined whether the reduction in oxidative stress translated into improved cellular function. In HUVECs, SC significantly impaired metabolic viability at 48 h, whereas Rapalink-1 alone or in combination with SC preserved viability. Similarly, in SMCs, SC exposure reduced cellular viability, while Rapalink-1 co-treatment restored viability to near-control levels (Figure 1C,D).

2.2. Rapalink-1 Attenuates SC-Induced DNA Damage and Oxidative DNA Lesions in Vascular Cells

Because oxidative stress and genotoxic injury are closely linked, we next evaluated DNA damage using γ-H2AX and 8-OHDG staining.

In line with the ROS expression data, SC provoked a clear increase in DNA damage in HUVECs, as indicated by elevated γ-H2AX positivity, which was significantly attenuated by treatment in combination with Rapalink-1 (Percentage of positive cells: Control = 13.69 ± 3.62%; SC = 32.24 ± 4.03%; Rapalink-1 = 18.66 ± 0.49%; SC + Rapalink-1 = 21.13 ± 1.21%; $p = 0.0002$; Figure 2A,B).

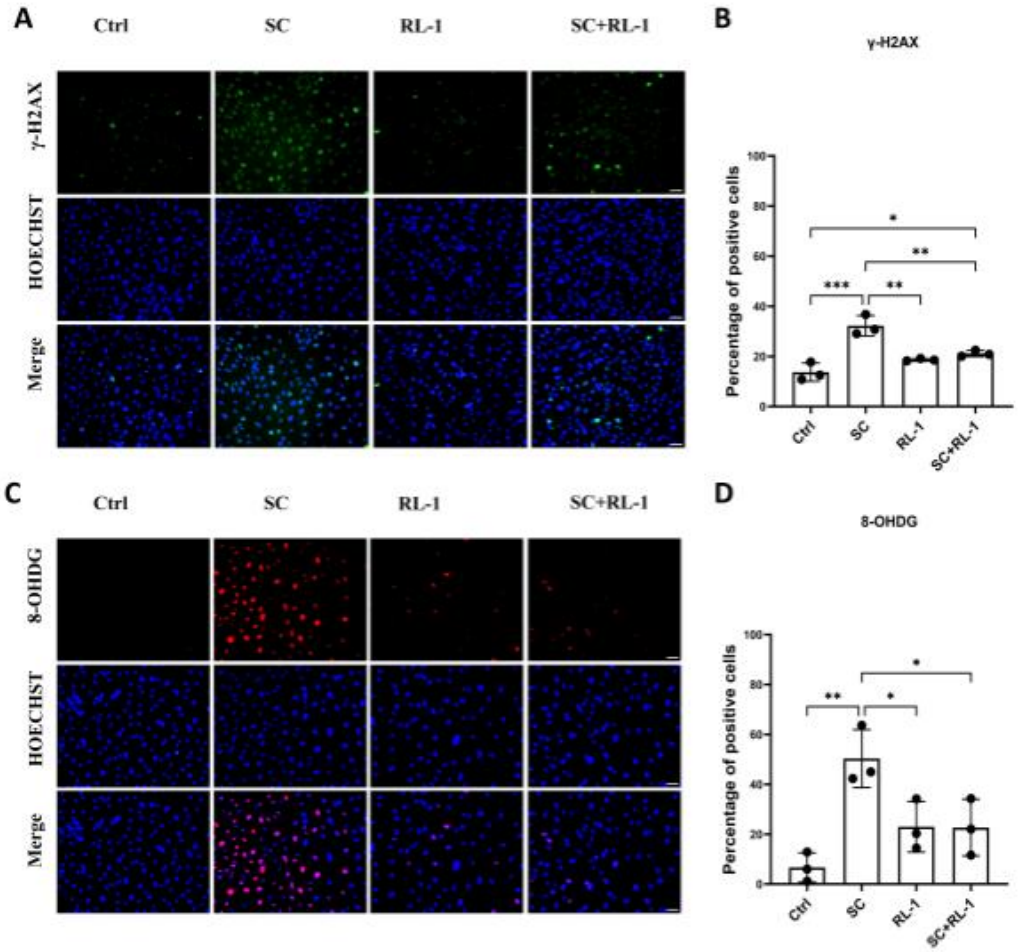

Figure 2. (**A**) Representative immunofluorescence images showing γ-H2AX (green), nuclei (Hoechst, blue) and merged images in HUVECs after 2 h treatment under the indicated conditions (Ctrl, SC, RL-1, and SC + RL-1). (**B**) Quantification of γ-H2AX staining. (**C**) Representative immunofluorescence images showing 8-OHDG (red), nuclei (Hoechst, blue) and merged images in HUVECs after 2 h treatment under the indicated conditions. (**D**) Quantification of 8-OHDG staining. Scale bar = 50 µm. Data are presented as mean ± SD ($n = 3$). Statistical significance was determined using one-way ANOVA with Tukey's post hoc test. Significance is indicated as: * $p < 0.05$, ** $p < 0.01$, *** $p < 0.001$.

We next assessed oxidative DNA base lesions using 8-OHDG. SC markedly increased the proportion of 8-OHDG-positive cells, which was reversed by Rapalink-1 treatment (Percentage of positive cells: Control = 6.66 ± 5.89%; SC = 50.30 ± 11.62%; Rapalink-1 = 22.97 ± 10.12%; SC + Rapalink-1 = 22.64 ± 11.35%; $p = 0.0047$; Figure 2C,D).

The corresponding experiments in SMCs yielded comparable trends and are provided in Supplementary Figure S2.

2.3. Rapalink-1 Alleviates SC-Induced Premature Senescence

Oxidative stress and DNA damage are well-established drivers of cellular senescence; accordingly, we assessed SA-β-gal activity, Lamin B1 expression, and p21, and found consistent senescence-associated changes in both HUVECs and SMCs.

In HUVECs, SC markedly increased the proportion of SA-β-gal–positive cells, whereas Rapalink-1 alone induced only a mild change; importantly, treatment in combination with Rapalink-1 significantly suppressed SC-induced senescence (Percentage of SA-β-gal–positive cells: Control = 1.32 ± 0.47%; SC = 14.81 ± 2.53%; Rapalink-1 = 3.71 ± 2.64%; SC + Rapalink-1 = 3.81 ± 2.27%; $p = 0.0003$; Figure 3A,B).

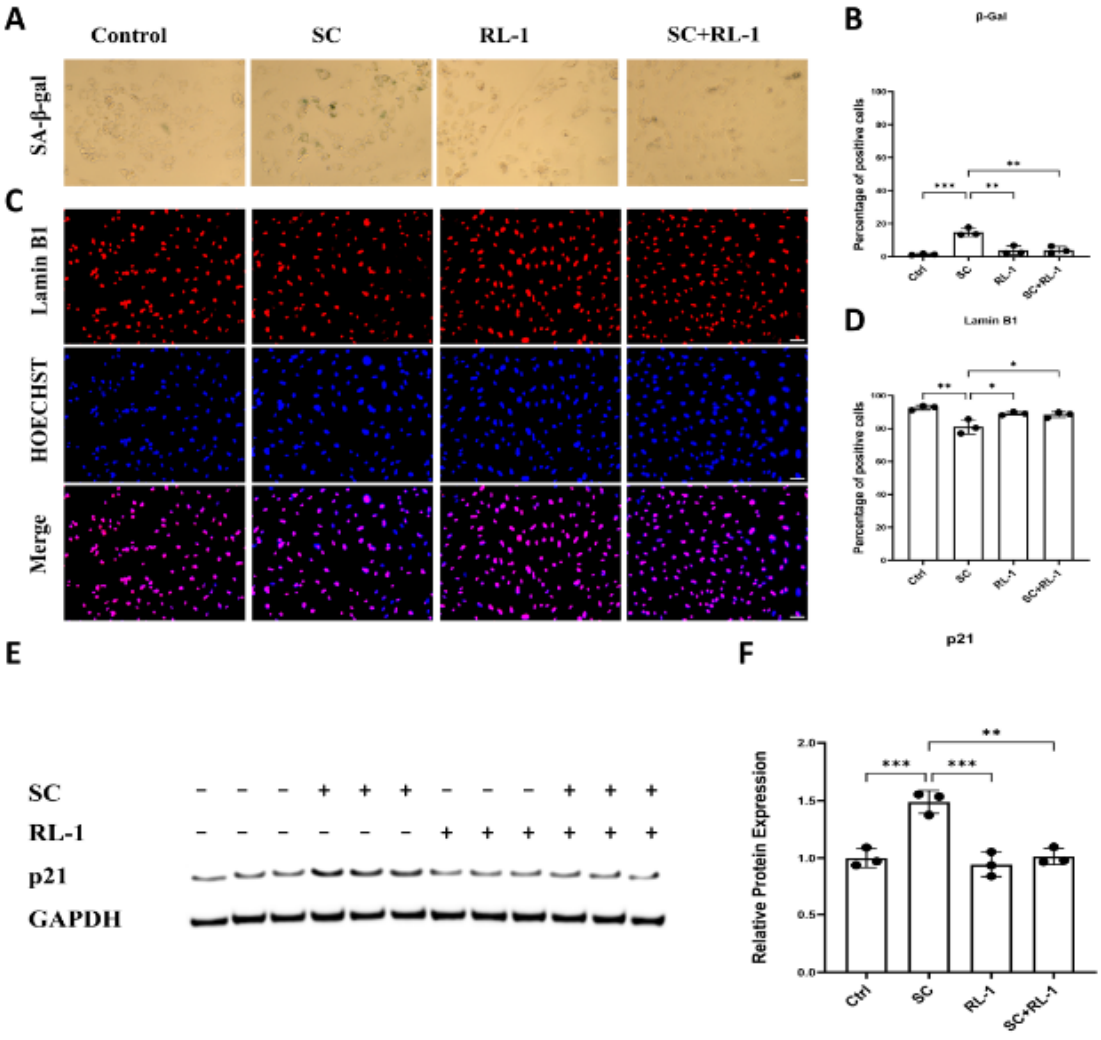

Figure 3. (**A**) Representative images of SA-β-gal staining in HUVECs after 24 h treatment under Control, SC, RL-1, and SC + RL-1 conditions. (**B**) Quantification of SA-β-gal-positive cells. (**C**) Representative immunofluorescence images of Lamin B1 (red), Hoechst nuclear counterstaining (blue) and merged images in HUVECs after 24 h treatment. (**D**) Quantification of Lamin B1-positive cells. (**E**) Representative immunoblotting of p21 expression after 24 h treatment. (**F**) Densitometric analysis of p21 protein levels normalized to GAPDH. Scale bar = 50 μm. Data are presented as mean ± SD ($n = 3$). Statistical significance was determined using one-way ANOVA with Tukey's post hoc test. Significance is indicated as: * $p < 0.05$, ** $p < 0.01$, *** $p < 0.001$.

Consistent with a senescent phenotype, SC exposure led to a pronounced reduction in Lamin B1 positivity, which was effectively preserved by treatment in combination with Rapalink-1 (Percentage of Lamin B1–positive cells: Control = 92.69 ± 1.41%;

SC = 81.04 ± 4.37%; Rapalink-1 = 89.15 ± 1.04%; SC + Rapalink-1 = 88.43 ± 1.74%; $p = 0.0029$; Figure 3C,D).

To further confirm senescence-associated growth arrest, we examined p21 protein levels by Western blotting. SC significantly upregulated p21 expression, whereas Rapalink-1 attenuated this induction in the SC + Rapalink-1 group (Figure 3E,F).

In SMCs, SA-β-gal staining did not show a consistent increase following SC treatment and was therefore not used as the primary readout of senescence in this cell type. Instead, senescence-associated changes were supported by the reduction of Lamin B1 and the induction of p21, both of which were attenuated by Rapalink-1 co-treatment (Supplementary Figure S3).

2.4. Rapalink-1 Attenuates SC-Induced SASP-Associated Inflammatory and ECM Remodeling Responses

To further evaluate the effects of Rapalink-1 on the senescence-associated secretory phenotype (SASP) and extracellular matrix (ECM) remodeling, we assessed transcriptional changes in key inflammatory and matrix-related genes in HUVECs and SMCs.

Analysis of the qPCR data showed that Rapalink-1 attenuated several SC-induced transcriptional changes associated with inflammatory/SASP- and matrix-remodeling responses. Representative HUVEC data are shown in Figure 4A–H, in which Rapalink-1 reduced the SC-induced upregulation of TNF-α, ICAM1, MMP1, MMP10, and TIMP3, whereas PTGS2 remained elevated despite Rapalink-1 treatment. MMP11 showed only modest changes, and TIMP4 showed a downward trend in the SC + RL-1 group. Given the prominent ECM-related changes in SMCs, selected SMC ECM-associated transcripts (COL1A1, EFEMP1, and ELN) are shown in Figure 4I–K. The full qPCR results for HUVECs and SMCs are provided in Tables 1 and 2, and an overview heatmap comparing SC + Rapalink-1 versus SC is presented in Supplementary Figure S4. Notably, the magnitude and direction of regulation differed between HUVECs and SMCs, indicating cell-type-specific responses.

To provide representative protein-level support for selected SASP/ECM-associated alterations, we performed Western blot analysis of MMP-2 and VCAM-1 in both HUVECs and SMCs. Additional qPCR data for selected markers, including MMP2 and VCAM1, are provided in Supplementary Table S3. SC significantly increased the protein expression of MMP-2 and VCAM-1, whereas treatment in combination with Rapalink-1 reduced their expression toward control levels. Representative data from HUVECs are shown in the main figures, while corresponding analyses in SMCs are provided in the Supplementary Information (Supplementary Figure S4).

2.5. Rapalink-1 Modulates NF-κB- and MAPK-Related Signaling and Alters Downstream mTOR-Related Readouts

Oxidative stress is a major trigger of inflammatory signaling in vascular cells. We therefore assessed NF-κB- and MAPK-related signaling by measuring total and phosphorylated p65, p38, and ERK1/2 in HUVECs and SMCs under the indicated conditions.

In HUVECs, SC was associated with increased abundance of p-p65, p-p38, and p-ERK, and these phospho-signals were reduced in the presence of Rapalink-1 (Figure 5A–D). The attenuation was most evident for p-p65 and p-p38, whereas p-ERK also showed a decrease in the SC + RL-1 group. As phosphorylation-dependent changes are commonly used as readouts of NF-κB- and MAPK-related signaling, phosphorylated proteins were used as the principal readouts, while the corresponding total proteins were also assessed to support interpretation.

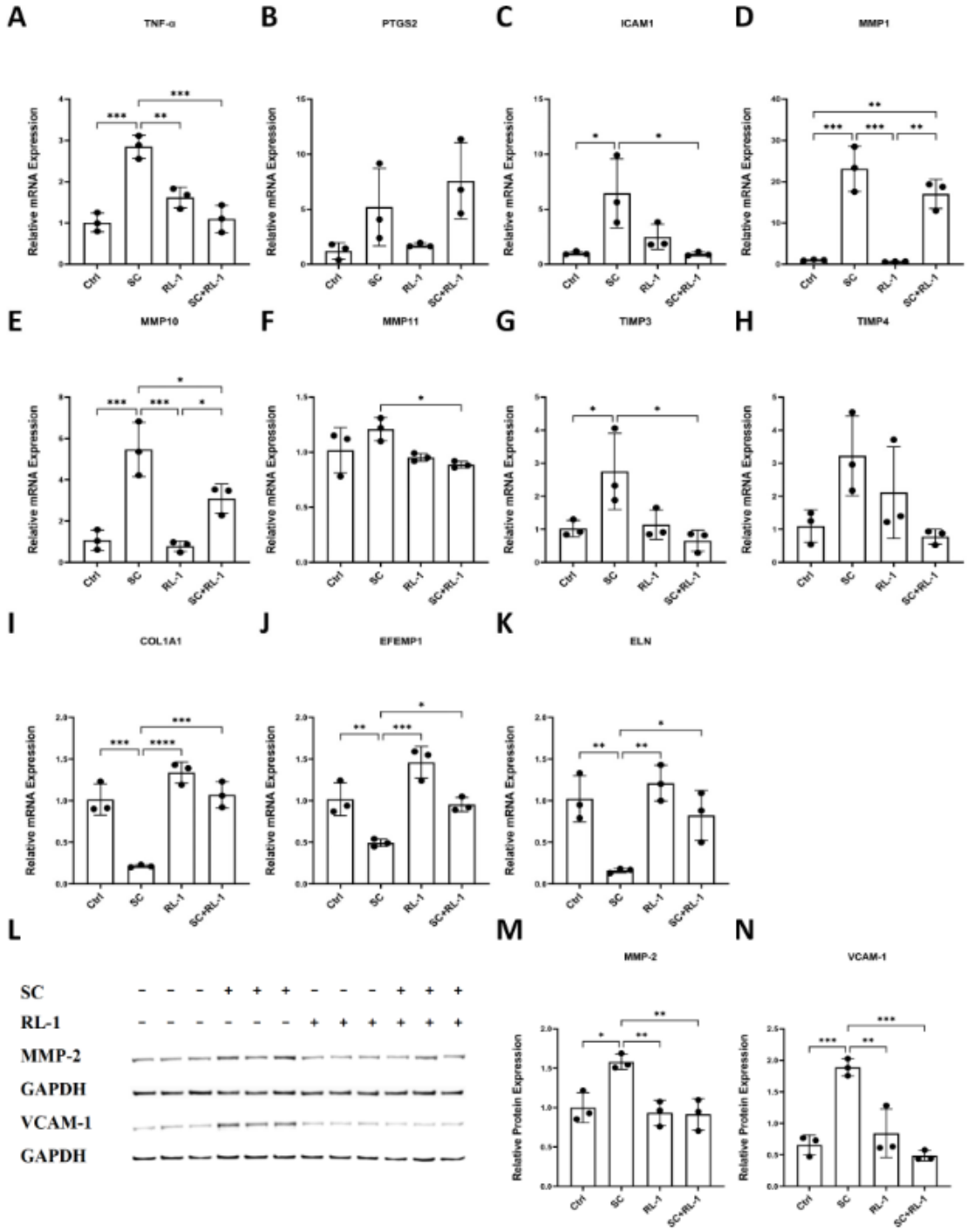

Figure 4. (**A**–**H**) Relative mRNA expression of TNF-α, PTGS2, ICAM1, MMP1, MMP10, MMP11, TIMP3, and TIMP4 in HUVECs after 24 h treatment. (**I**–**K**) Relative mRNA expression of selected ECM-associated genes (Collagen1, Fibulin3, and ELN) in SMCs after 24 h treatment. (**L**) Representative immunoblots of MMP-2 and VCAM-1 in HUVECs after 24 h treatment, with GAPDH as the loading control. (**M**,**N**) Quantification of MMP-2 and VCAM-1 protein expression normalized to GAPDH in HUVECs. Data are presented as mean ± SD ($n = 3$). Statistical significance was determined using one-way ANOVA with Tukey's post hoc test. Significance is indicated as: * $p < 0.05$, ** $p < 0.01$, *** $p < 0.001$, **** $p < 0.0001$.

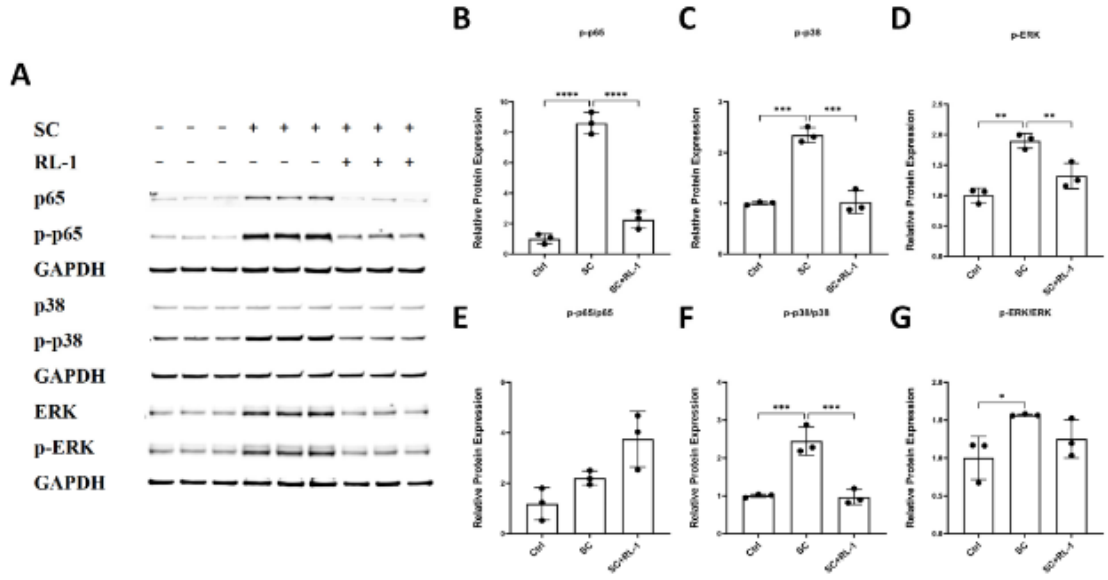

Figure 5. (**A**) Representative blots of the indicated proteins in HUVECs after 24 h treatment. (**B**–**G**) Quantification of the relative protein expression of p-p65, p-p38, p-ERK, p-p65/p65, p-p38/p38 and p-ERK/ERK in HUVECs. Protein expression was normalized to GAPDH. Data are presented as mean ± SD ($n = 3$). Statistical significance was determined using one-way ANOVA with Tukey's post hoc test. Significance is indicated as: * $p < 0.05$, ** $p < 0.01$, *** $p < 0.001$, **** $p < 0.0001$.

Among the phospho/total ratios, p-p38/p38 showed a pattern broadly consistent with the phospho-protein abundance data, whereas the corresponding ratios for p65 and ERK were less clearly aligned with the changes observed in phospho-protein abundance alone (Figure 5E–G), suggesting that SC and Rapalink-1 may influence both phosphorylation state and total protein abundance in a target-dependent manner. Overall, these findings support modulation of NF-κB- and MAPK-related signaling by Rapalink-1 in HUVECs. Comparable trends were also observed in SMCs and are presented in the Supplementary Information (Supplementary Figure S5).

Because Rapalink-1 is a dual mTORC1/2 inhibitor, we next examined pathway activity to confirm on-target signaling modulation in HUVECs and SMCs. Notably, neither total mTOR nor phosphorylated mTOR levels showed significant differences among groups, and the p-mTOR/mTOR ratio remained unchanged (Supplementary Figure S6), suggesting that SC does not measurably alter mTOR phosphorylation status at this time point. We therefore focused on downstream pathway outputs. Immunoblotting revealed that SC activated S6 signaling, whereas Rapalink-1 attenuated this response. Specifically, p-S6 levels were elevated following SC exposure and decreased upon Rapalink-1 treatment (Figure 6A,B). Notably, the p-S6/S6 ratio did not show a significant difference among groups, suggesting that the overall increase in p-S6 was largely accompanied by changes in total S6 abundance rather than a marked shift in phosphorylation stoichiometry (Figure 6C). These findings suggest that SC may regulate mTOR pathway output primarily at the level of downstream effectors rather than through detectable changes in mTOR phosphorylation.

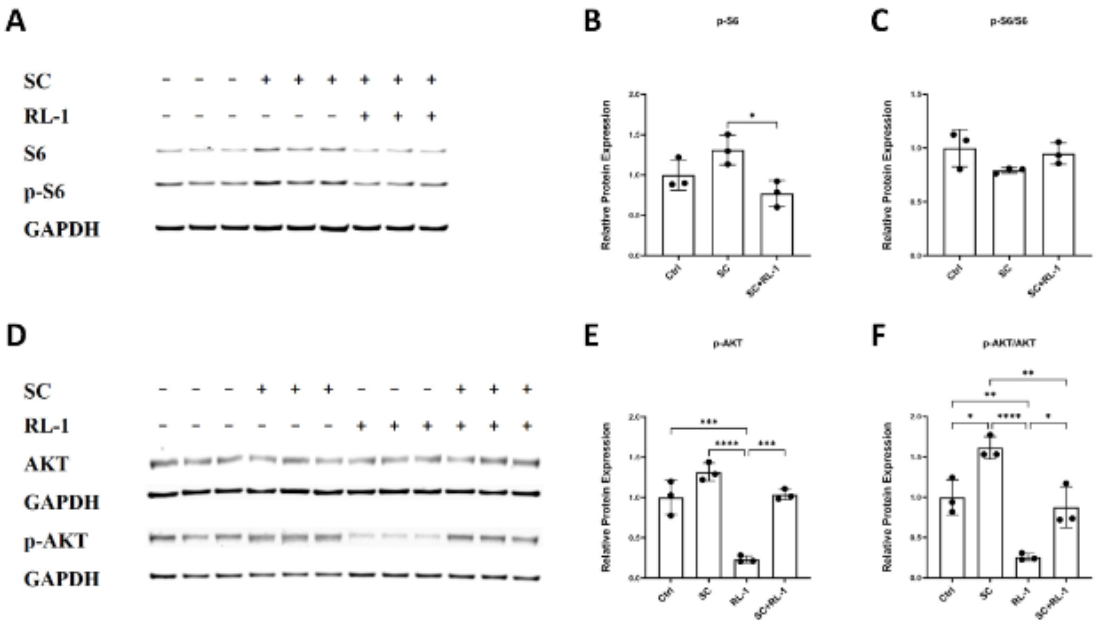

Figure 6. (**A**) Representative immunoblot images showing total S6, phospho-S6 (p-S6) and GAPDH in HUVECs after 24 h treatment. (**B**,**C**) Quantification of relative protein expression levels of p-S6, and the p-S6/S6 ratio. (**D**) Representative immunoblot images for AKT and p-AKT in HUVECs after 24 h treatment. (**E**,**F**) Quantification of p-AKT and p-AKT/AKT ratio. Protein expression was normalized to GAPDH. Data are presented as mean ± SD ($n = 3$). Statistical significance was determined using one-way ANOVA with Tukey's post hoc test. Significance is indicated as: * $p < 0.05$, ** $p < 0.01$, *** $p < 0.001$, **** $p < 0.0001$.

AKT-related signaling was assessed by measuring p-AKT and the p-AKT/AKT ratio. SC increased p-AKT levels in HUVECs, whereas Rapalink-1 alone markedly reduced p-AKT and SC + RL-1 partially attenuated the SC-associated increase (Figure 6D,E). SC also significantly increased the p-AKT/AKT ratio in HUVECs, while Rapalink-1 alone markedly suppressed this ratio. Importantly, co-treatment with Rapalink-1 partially reversed SC-induced AKT activation, restoring p-AKT/AKT toward baseline levels (Figure 6D,F). SMCs exhibited a comparable pattern of S6 and AKT pathway modulation; however, these data are presented in the Supplementary Figures (Supplementary Figure S5).

Collectively, these results indicate that SC enhances downstream mTOR-related signaling in both HUVECs and SMCs, whereas Rapalink-1 attenuates this pathway activation despite minimal detectable changes in mTOR phosphorylation itself.

3. Discussion

Cigarette smoking accelerates vascular aging and degeneration through complex, interdependent mechanisms involving oxidative stress, inflammation, and ECM remodeling [1–4,32]. Although each of these processes has been linked to smoking-related vascular pathology, how they converge at the cellular signaling level remains incompletely defined [32,33]. Here, we show that SC induces a coordinated stress-associated phenotype in vascular cells and dual mTORC1/2 inhibition with Rapalink-1 attenuates several linked components of this response.

A central observation of this study is that oxidative stress is closely linked to downstream genotoxic injury and senescence establishment following smoke exposure. SC induced a rapid increase in intracellular ROS in HUVECs [21–23,34]. This oxidative burst was accompanied by a broader reprogramming of redox-responsive genes, including induction of oxidant-generating and antioxidant defense pathways [5–7,12]. Comparable

oxidative responses were also observed in SMCs, supporting the view that smoke-induced redox stress is not restricted to endothelial cells.

Consistent with an oxidative-to-genotoxic progression, SC exposure was associated with accumulation of canonical DNA damage markers in HUVECs, including increased γ-H2AX positivity and elevated 8-OHDG, indicative of DNA damage signaling and oxidative DNA base lesions, respectively [12,14–16,24]. Similar trends in SMCs further support the generalizability of this oxidative–genotoxic axis. Mechanistically, oxidative and genotoxic stress are known to reinforce one another: persistent ROS can induce DNA lesions and mitochondrial dysfunction, while unresolved DNA damage activates the DNA damage response (DDR) and checkpoint pathways that promote stable growth arrest [14–16,33,35]. When stress is sustained, this state can transition into irreversible senescence, which is further stabilized by nuclear and chromatin remodeling, including depletion of Lamin B1 and reinforcement of inflammatory transcriptional programs that underpin SASP outputs [36]. In this framework, SC-induced increases in SA-β-gal activity, Lamin B1 loss, and induction of p21 protein are consistent with DDR-associated senescent growth arrest in our model.

Notably, Rapalink-1 attenuated this upstream oxidative–genotoxic cascade at multiple levels. Co-treatment significantly reduced SC-induced ROS accumulation. This effect was accompanied by a partial restoration of cellular viability under smoke stress and blunting of the maladaptive redox-responsive transcriptional activation pattern, suggesting that mTOR-centered signaling may influence oxidant burden and/or redox compensation under smoke stress [25–28,31,37]. An exception was HMOX1 in HUVECs, which remained elevated despite Rapalink-1 co-treatment, suggesting that the effects of Rapalink-1 are selective rather than uniformly suppressive, possibly preserving aspects of adaptive cytoprotective signaling while dampening maladaptive stress amplification. In parallel, Rapalink-1 decreased γ-H2AX and 8-OHDG signals, indicating reduced downstream DNA damage. At the phenotypic level, Rapalink-1 suppressed senescence-associated features, including reduced SA-β-gal positivity, preservation of Lamin B1, and diminished induction of p21 protein. Together, these findings are consistent with the interpretation that dual mTORC1/2 inhibition can decouple smoke-induced oxidative stress from subsequent genotoxic injury and senescence stabilization in vascular cells challenged by tobacco-derived toxins.

A major pathological consequence of vascular senescence is the emergence of SASP-associated programs that can amplify chronic inflammation and promote ECM remodeling [14,15,17,35]. In this context, senescence and SASP are mechanistically coupled: persistent stress signaling that establishes senescence also supports sustained inflammatory transcriptional output that reinforces and propagates tissue dysfunction. Consistent with this model, SC induced broad upregulation of SASP-associated transcripts in vascular cells [17,18,38,39]. Importantly, these transcriptional changes were accompanied by signatures consistent with adverse tissue remodeling: SC reduced expression of key structural ECM genes such as ELN, collagen1, and fibulin3, whereas Rapalink-1 partially restored these transcripts toward control levels [18,39,40]. Rapalink-1 also reduced SC-induced expression of representative inflammatory/ECM-associated effectors at the protein level (e.g., MMP-2 and VCAM-1). Collectively, these data suggest that Rapalink-1 not only attenuates senescence-associated cellular phenotypes but also modulates downstream SASP-associated inflammatory and ECM-related molecular changes induced by SC. This raises the possibility that the effect of Rapalink-1 is not limited to reducing cellular injury, but may also involve reshaping the secretory and inflammatory phenotype of stressed vascular cells, in line with the recognized role of mTOR in SASP regulation.

Mechanistically, our data implicate coordinated suppression of NF-κB and MAPK signaling as a key node through which Rapalink-1 dampens smoke-induced inflammatory transcription and SASP-associated outputs. NF-κB and MAPK pathways are well-

established drivers of inflammatory gene expression and are strongly implicated in maintaining SASP-related programs [41–45].

In our study, SC was associated with increased abundance of phosphorylated p65 (NF-κB), p38, and ERK (MAPK), whereas Rapalink-1 reduced these phosphorylation-related readouts in HUVECs. Comparable pathway modulation was observed in SMCs, supporting a conserved mechanism across vascular cell types. These signaling effects provide a plausible mechanistic basis for the broad suppression of SASP-associated transcripts and the partial preservation of ECM-related gene expression, and suggest that dual mTORC1/2 inhibition disrupts a self-reinforcing circuit linking stress signaling, inflammatory transcription, and senescence/SASP maintenance. The relationship between cigarette smoke exposure and mTOR signaling is likely context-dependent rather than uniformly activating. In this regard, previous work in pulmonary injury models identified RTP801/REDD1, a suppressor of mTOR signaling, as an essential mediator of cigarette smoke-induced injury, suggesting that smoke exposure can also engage mTOR-inhibitory stress programs in a tissue- and model-specific manner [46]. Against this background, the present findings are best interpreted as evidence for modulation of selected downstream mTOR-related signaling readouts in vascular cells under the current experimental conditions rather than a universal pattern of canonical mTOR activation by smoke.

An additional aspect of our findings is the modulation of AKT signaling by Rapalink-1 under smoke stress. SC exposure increased the p-AKT/AKT ratio, consistent with engagement of adaptive pro-survival signaling in response to sustained cellular stress, whereas Rapalink-1 alone reduced basal AKT activity; notably, co-treatment partially normalized stress-induced AKT activation toward baseline levels [25,26,47–49]. In parallel, Rapalink-1 reduced SC-associated p-S6 abundance, supporting on-target modulation of downstream mTOR-related signaling. This bidirectional tuning of AKT output may be relevant in senescence biology, where excessive survival signaling can stabilize senescent cells and reinforce SASP programs, whereas overly aggressive suppression could compromise viability. Thus, dual mTORC1/2 inhibition may recalibrate adaptive AKT signaling while restraining pathological inflammatory and metabolic pathway activation.

Taken together with previous studies, our findings support the view that vascular senescence is one of the mechanisms linking cigarette smoke exposure to vascular injury and degeneration [12–16,32,33,35,50]. Rather than causing only acute cellular damage, cigarette smoke may impose sustained oxidative and inflammatory stress on the vessel wall, thereby promoting endothelial dysfunction and genotoxic injury [5–8,34,50–52]. When such stress persists, vascular cells may acquire a senescence-associated phenotype characterized by growth arrest and phenotypic remodeling [14–16,33,36]. In turn, these cells may develop a SASP-associated inflammatory profile together with ECM-remodeling changes, which can further disturb vascular homeostasis and amplify local tissue injury [14,15,17,18,38,39].

In this context, oxidative stress, DNA damage, cellular senescence, and maladaptive matrix remodeling are better viewed as interconnected processes rather than isolated events [32,33,35,38,39,50]. Their interaction is likely to contribute to vascular aging and may be relevant to smoking-related vascular diseases, including atherosclerotic change and aneurysm-associated wall degeneration [3,4,9–11,32,39,52]. Our study may provide mechanistic support for the idea that targeting senescence-associated signaling pathways may help limit smoke-induced vascular injury and may be relevant to strategies aimed at preserving vascular health during aging [20,30,31].

Several limitations should be acknowledged. This study was performed in vitro using cultured endothelial and smooth muscle cells and therefore does not fully recapitulate the biomechanical, immune, and hemodynamic complexity of the vascular wall in vivo. Future studies employing animal models of chronic smoke exposure and vascular disease will

be needed to validate these findings and assess the long-term safety and efficacy of dual mTORC1/2 inhibition.

4. Materials and Methods

4.1. Cell Culture

The HUVEC models were procured from PromoCell (Heidelberg, Germany). Endothelial cell medium (C-22210, PromoCell, Heidelberg, Germany) containing endothelial growth factors (C-39215, PromoCell, Heidelberg, Germany) was used to maintain the HUVECs at 37 °C in a humidified environment with 5% CO_2. The SMC models were procured from PromoCell (Heidelberg, Germany). Smooth muscle cell medium (C-22262) supplemented with smooth muscle growth factors (C-39267) was used to maintain SMCs at 37 °C in 5% CO_2. Upon arrival, the cells were thawed and seeded in T75 culture flasks. The cells were passaged when they reached 80–90% confluence. For passaging, the cells were washed with PBS and incubated with trypsin for 4 min at 37 °C and 5% CO_2. The cells were seeded at a density of 5000 cells/cm^2 in new cell culture plates. All experiments with HUVECs and SMCs were performed at passage 7. All experiments were performed with three biological replicates.

4.2. Tobacco Smoke Condensate Preparation

Tobacco smoke condensate (SC) was prepared by smoking commercial cigarettes on an automated smoking machine following standard procedures for mainstream smoke collection. The smoke was passed through a Cambridge filter pad to collect the particulate phase. The pad was extracted with absolute ethanol, and the solvent was evaporated under a gentle nitrogen stream at room temperature. The dried residue was weighed and dissolved in DMSO to prepare a 100 mg/mL stock solution. For cell exposure, the stock was diluted in culture medium to the desired concentrations (final DMSO $\leq$ 0.1% v/v).

4.3. MTT Assay

Cell viability was evaluated using the MTT (3-(4,5-dimethylthiazol-2-yl)-2,5-diphenyltetrazolium bromide) assay. HUVECs and SMCs were seeded in 96-well plates at a density of 5000 cells/cm^2 and incubated overnight at 37 °C in a humidified atmosphere with 5% CO_2 to allow for cell attachment. The next day, the culture medium was replaced with fresh medium containing tobacco smoke condensate (50 µg/mL), 200 pM Rapalink-1, or a combination of tobacco smoke condensate and Rapalink-1. The concentrations used in the present study (SC: 50 µg/mL; Rapalink-1: 200 pM) were chosen based on previous studies and empirical observations under our experimental conditions. Cells cultured in drug-free medium served as the control group. After 24 and 48 h of treatment, 10 µL of MTT solution (5 mg/mL in PBS) was added to each well, and cells were incubated for an additional 3–4 h at 37 °C. Following incubation, the culture medium was carefully removed, and 100–150 µL of DMSO was added to dissolve the formazan crystals. Cell viability was assessed by measuring the optical density (OD) at 550 nm with reference at 655 nm. Background values were subtracted. All experiments were performed in triplicate.

4.4. DCFH-DA Staining

To investigate the accumulation of cellular ROS, 5000 cells/cm^2 HUVECs and SMCs were seeded in a 96-well plate. The next day, the medium was replaced with fresh medium either containing tobacco smoke condensate (50 µg/mL), 200 pM Rapalink-1 or tobacco smoke condensate combined with Rapalink-1. HUVECs and SMCs medium alone was used as a control. After 2 h of treatment, 10 µM of the fluorescence probe 2,7-dichlorofluorescein diacetate (DCFH-DA, D6883, Sigma-Aldrich, St. Louis, MO, USA) was added to the

cells. The cells were incubated with DCFH-DA at 37 °C for 30 min in the dark. The cells were washed three times with a serum-free medium. After DCFH-DA incubation and washing, the nuclei were counterstained with Hoechst. Images were acquired using identical microscope settings for all groups within each experiment and analyzed using ImageJ (version 1.53c; National Institutes of Health, Bethesda, MD, USA). DCF-positive cells were quantified relative to the total number of Hoechst-positive nuclei in the same field.

4.5. Immunofluorescence Staining

The cells were treated with different conditions (as described in the previous section) for 2 h for 8-OHDG, γ-H2AX staining and 24 h for Lamin B1 staining. After washing cells thrice with PBS, the cells were fixed with 4% paraformaldehyde for 10 min at RT. After washing cells thrice with PBS, for permeabilization, the cells were treated with 0.2% Triton™ X-100 at RT for 10 min. For blocking, the cells were incubated with 5% bovine serum albumin (BSA) at RT for 1 h. The cells were incubated overnight with primary antibodies 8-OHDG, γ-H2AX and Lamin B1 (Supplementary Table S1) at 4 °C. The next day, after washing cells thrice with PBS, the cells were incubated with secondary antibodies (Supplementary Table S1) for 1 h at RT. Hoechst (Sigma-Aldrich) was used for nuclear staining. The images were captured using a Leica DMi8 Inverted Microscope and the compatible LAS-X Life Science Microscope Software, version 3.7.5.24914 (Leica Application Suite X) Platform. All immunofluorescence experiments were independently repeated three times, with triplicate wells per condition in each experiment. One predefined central field was captured from each well using identical imaging settings within each experiment. Images were processed in Fiji/ImageJ (version 1.53c) (National Institutes of Health, Bethesda, MD, USA) using identical brightness/contrast settings. Positive cells were manually counted in a masked manner and expressed as a percentage of the total number of Hoechst-positive nuclei in the same field.

4.6. Western Blot

For protein analysis, cells were treated with tobacco smoke condensate (50 µg/mL) or tobacco smoke condensate combined with Rapalink-1 for 24 h. Untreated HUVECs and SMCs were used as controls. RIPA buffer was used for total protein extraction. DC Protein Assay Kit (500-0116, Bio-Rad, Hercules, CA, USA) was used to quantify protein concentration. Subsequently, 30 µg of total protein under reducing conditions was loaded onto a 12% sodium dodecyl sulfate-polyacrylamide gel. For the first 10 min, electrophoresis was conducted at 60 Volts, followed by 90 Volts for 60–90 min. The separated proteins were then transferred onto a 0.45 µm pore-size nitrocellulose membrane at 250 mA for 120 min. The membranes were blocked for one hour with a 5% bovine serum albumin (BSA) solution in 0.05% TBST to minimize nonspecific binding. After that, the membranes were incubated with primary antibodies (see Supplementary Table S1) in 5% BSA overnight at 4 °C on a shaking platform. Afterward, the membranes underwent 3 × 10 min washes with TBST and were subsequently exposed to secondary antibodies diluted in 0.05% TBST (refer to Supplementary Table S1) for one hour at room temperature. Densitometric analysis was performed using NIH ImageJ. For protein-abundance plots, target protein signals were normalized to GAPDH. Where indicated, phospho/total ratios were calculated separately from the corresponding phospho- and total-protein signals. Depending on the specific experiment, Western blot analyses were performed using either four treatment groups (Control, SC, Rapalink-1, and SC + Rapalink-1) or three groups (Control, SC, and SC + Rapalink-1).

4.7. Quantitative Polymerase Chain Reaction (qPCR)

For qPCR analysis, cells were treated with tobacco smoke condensate (50 µg/mL), 200 pM Rapalink-1, or tobacco smoke condensate combined with Rapalink-1 for 24 h. Total RNA was extracted using the Nucleo Spin RNA kit (740955.50, MACHEREY-NAGEL, Düren, Germany) according to the manufacturer's instructions. A total of 1.2 µg of RNA was utilized for reverse transcription, accomplished using the MMLV Reverse Transcriptase kit (M1701, Promega, Walldorf, Germany), Random Hexamer Primers (48190011, Thermo Fisher Scientific, Waltham, MA, USA), and RiboLock RNase Inhibitor (EO0384, Thermo Fisher Scientific Baltics UAB, Vilnius, Lithuania). The qPCR was run using total cDNA combined with AceQ SYBR qPCR Master Mix (Q111-03, Vazyme, Nanjing, China) and primers (Supplementary Table S2) on a QuantStudio™ 3 Real-Time PCR Instrument (Applied Biosystems, Thermo Fisher Scientific, Waltham, MA, USA). The thermal cycling program consisted of an initial denaturation step at 95 °C for 8 min, followed by 40 cycles of 95 °C for 15 s, 58.9 °C for 30 s, and 72 °C for 30 s, concluding with a melting curve analysis. The relative mRNA expressions were calculated by the $2^{-\Delta\Delta Ct}$ method using β-actin as the reference.

4.8. Senescence-Associated β-Galactosidase Staining

For senescence-associated beta-galactosidase (β-Gal) staining, cells were treated for 24 h as described in the previous sections. SA β-Gal staining was performed using the Senescence Cells Histochemical Staining Kit (GALS, Sigma, St. Louis, MO, USA) following the manufacturer's instructions. The cells were incubated with SA-β-galactosidase staining solution at 37 °C for seven hours. The staining solution was aspirated and the cells were overlaid with 70% glycerol in PBS. After staining, the cells were stored at 4 °C. The images were captured using a Leica DMi8 Inverted Microscope and the compatible LAS-X Life Science Microscope Software version 3.7.5.24914 (Leica Application Suite X) Platform. SA-β-gal staining experiments were independently repeated three times, with triplicate wells per condition in each experiment. One predefined central field was captured from each well using identical imaging settings. Positive cells were manually counted in a masked manner relative to the total number of cells in the same field.

4.9. Statistical Analysis

Statistical analyses were performed using GraphPad Prism (version 10.1.2). Comparisons among groups were conducted using one-way ANOVA followed by Tukey's post hoc test. For experiments repeated independently three times, data from triplicate wells within each experiment were averaged before statistical analysis.

5. Conclusions

Our study demonstrates that Rapalink-1 attenuates SC-induced oxidative stress, DNA damage, senescence-associated changes, and inflammatory/ECM-related molecular responses in vascular endothelial and smooth muscle cells in vitro. These findings support Rapalink-1 as a candidate modulator of smoke-induced vascular aging and senescence-associated remodeling, warranting further validation in disease-relevant models of vascular aging and in vivo studies.

Supplementary Materials: The following supporting information can be downloaded at: https://www.mdpi.com/article/10.3390/ijms27083636/s1.

Author Contributions: Conceptualization: S.M.; Methodology: J.Y. and S.M.; Data collection and curation: J.Y., R.M. and H.L.; Formal analysis and investigation: J.Y.; Writing—original draft preparation:

J.Y.; Writing—review and editing: S.M., D.K., R.M. and K.F.; Funding acquisition: S.M.; Resources: S.M.; Supervision: S.M. All authors have read and agreed to the published version of the manuscript.

Funding: This research was funded by the China Scholarship Council Grant No. 202408080196.

Institutional Review Board Statement: Not applicable.

Informed Consent Statement: Not applicable.

Data Availability Statement: The original contributions presented in this study are included in the article/Supplementary Material. Further inquiries can be directed to the corresponding author.

Acknowledgments: The authors thank the members of the Department of Neurology, Medical Faculty, University Hospital Düsseldorf, for technical assistance.

Conflicts of Interest: The authors declare no conflicts of interest.

Abbreviations

The following abbreviations are used in this manuscript:

8-OHDG	8-hydroxy-2′-deoxyguanosine
AKT	protein kinase B
BSA	bovine serum albumin
PTGS2	cyclooxygenase-2
DCFH-DA	2′,7′-dichlorofluorescein diacetate
DDR	DNA damage response
ECM	extracellular matrix
ERK	extracellular signal-regulated kinase (ERK1/2)
GAPDH	glyceraldehyde-3-phosphate dehydrogenase
HMOX1	heme oxygenase-1
HUVECs	human umbilical vein endothelial cells
ICAM-1	intercellular adhesion molecule-1
Lamin B1	Nuclear lamin B1
IF	immunofluorescence
NOS2	inducible nitric oxide synthase
MAPK	mitogen-activated protein kinase
SOD2	manganese superoxide dismutase (SOD2)
MMP(s)	matrix metalloproteinase(s)
mTOR	mechanistic target of rapamycin
MTT	3-(4,5-dimethylthiazol-2-yl)-2,5-diphenyltetrazolium bromide
NF-κB	nuclear factor kappa-light-chain-enhancer of activated B cells
NOX4	NADPH oxidase 4
NFE2L2	nuclear factor erythroid 2–related factor 2 (NFE2L2)
p21	Cyclin-dependent kinase inhibitor 1
P38	p38 mitogen-activated protein kinase (MAPK14)
p65	nuclear factor kappa B subunit p65 (RelA)
RIPA	radioimmunoprecipitation assay (buffer)
ROS	reactive oxygen species
RT	room temperature
SA-β-gal	senescence-associated β-galactosidase
SASP	senescence-associated secretory phenotype
SC	smoke condensate (tobacco smoke condensate)
SMCs	smooth muscle cells (vascular)
S6	ribosomal protein S6
TBST	Tris-buffered saline with Tween-20
TIMP(s)	tissue inhibitor(s) of metalloproteinases

TNF-α	tumor necrosis factor-alpha
γ-H2AX	phosphorylated H2A histone family member X (Ser139)
VCAM1	Vascular cell adhesion molecule 1

References

1. Ambrose, J.A.; Barua, R.S. The pathophysiology of cigarette smoking and cardiovascular disease. *J. Am. Coll. Cardiol.* **2004**, *43*, 1731–1737. [CrossRef]
2. Morris, P.B.; Ference, B.A.; Jahangir, E.; Feldman, D.N.; Ryan, J.J.; Bahrami, H.; El-Chami, M.F.; Bhakta, S.; Winchester, D.E.; Al-Mallah, M.H.; et al. Cardiovascular Effects of Exposure to Cigarette Smoke and Electronic Cigarettes. *J. Am. Coll. Cardiol.* **2015**, *66*, 1378–1391. [CrossRef] [PubMed]
3. Wang, H.; Wang, L.; Wang, J.; Zhang, L.; Li, C. The Biological Effects of Smoking on the Formation and Rupture of Intracranial Aneurysms: A Systematic Review and Meta-Analysis. *Front. Neurol.* **2022**, *13*, 862916. [CrossRef]
4. Hahad, O.; Arnold, N.; Prochaska, J.H.; Panova-Noeva, M.; Schulz, A.; Lackner, K.J.; Pfeiffer, N.; Schmidtmann, I.; Michal, M.; Beutel, M.; et al. Cigarette Smoking Is Related to Endothelial Dysfunction of Resistance, but Not Conduit Arteries in the General Population—Results from the Gutenberg Health Study. *Front. Cardiovasc. Med.* **2021**, *8*, 674622. [CrossRef]
5. Ungvari, Z.; Bailey-Downs, L.; Sosnowska, D.; Gautam, T.; Koncz, P.; Losonczy, G.; Ballabh, P.; de Cabo, R.; Sonntag, W.E.; Csiszar, A. Vascular oxidative stress in aging: A homeostatic failure due to dysregulation of NRF2-mediated antioxidant response. *Am. J. Physiol.-Heart Circ. Physiol.* **2011**, *301*, H363–H372. [CrossRef] [PubMed]
6. Loboda, A.; Damulewicz, M.; Pyza, E.; Jozkowicz, A.; Dulak, J. Role of Nrf2/HO-1 system in development, oxidative stress response and diseases: An evolutionarily conserved mechanism. *Cell. Mol. Life Sci.* **2016**, *73*, 3221–3247. [CrossRef] [PubMed]
7. Forstermann, U.; Sessa, W.C. Nitric oxide synthases: Regulation and function. *Eur. Heart J.* **2012**, *33*, 829–837. [CrossRef] [PubMed]
8. Pinnamaneni, K.; Sievers, R.E.; Sharma, R.; Selchau, A.M.; Gutierrez, G.; Nordsieck, E.J.; Su, R.; An, S.; Chen, Q.; Wang, X.; et al. Brief Exposure to Secondhand Smoke Reversibly Impairs Endothelial Vasodilatory Function. *Nicotine Tob. Res.* **2014**, *16*, 584–590. [CrossRef] [PubMed]
9. Etminan, N.; Rinkel, G.J. Unruptured intracranial aneurysms: Development, rupture and preventive management. *Nat. Rev. Neurol.* **2016**, *12*, 699–713. Erratum in *Nat. Rev. Neurol.* **2017**, *13*, 126. https://doi.org/10.1038/nrneurol.2017.14. [CrossRef] [PubMed]
10. Van Der Kamp, L.T.; Rinkel, G.J.E.; Verbaan, D.; Van Den Berg, R.; Vandertop, W.P.; Murayama, Y.; Ishibashi, T.; Lindgren, A.; Koivisto, T.; Teo, M.; et al. Risk of Rupture After Intracranial Aneurysm Growth. *JAMA Neurol.* **2021**, *78*, 1228. Erratum in *JAMA Neurol.* **2022**, *79*, 312. https://doi.org/10.1001/jamaneurol.2021.5146. [CrossRef] [PubMed]
11. Müller, T.B.; Vik, A.; Romundstad, P.R.; Sandvei, M.S. Risk Factors for Unruptured Intracranial Aneurysms and Subarachnoid Hemorrhage in a Prospective Population-Based Study. *Stroke* **2019**, *50*, 2952–2955. [CrossRef]
12. Nyunoya, T.; Monick, M.M.; Klingelhutz, A.; Yarovinsky, T.O.; Cagley, J.R.; Hunninghake, G.W. Cigarette Smoke Induces Cellular Senescence. *Am. J. Respir. Cell Mol. Biol.* **2006**, *35*, 681–688. [CrossRef]
13. Khan, D.; Zhou, H.; You, J.; Kaiser, V.A.; Khajuria, R.K.; Muhammad, S. Tobacco smoke condensate-induced senescence in endothelial cells was ameliorated by colchicine treatment via suppression of NF-κB and MAPKs P38 and ERK pathways activation. *Cell Commun. Signal.* **2024**, *22*, 214. [CrossRef]
14. Birch, J.; Gil, J. Senescence and the SASP: Many therapeutic avenues. *Genes Dev.* **2020**, *34*, 1565–1576. [CrossRef] [PubMed]
15. Tchkonia, T.; Zhu, Y.; Van Deursen, J.; Campisi, J.; Kirkland, J.L. Cellular senescence and the senescent secretory phenotype: Therapeutic opportunities. *J. Clin. Investig.* **2013**, *123*, 966–972. [CrossRef] [PubMed]
16. López-Otín, C.; Blasco, M.A.; Partridge, L.; Serrano, M.; Kroemer, G. The Hallmarks of Aging. *Cell* **2013**, *153*, 1194–1217. [CrossRef] [PubMed]
17. Coppé, J.-P.; Patil, C.K.; Rodier, F.; Sun, Y.; Muñoz, D.P.; Goldstein, J.; Nelson, P.S.; Desprez, P.-Y.; Campisi, J. Senescence-Associated Secretory Phenotypes Reveal Cell-Nonautonomous Functions of Oncogenic RAS and the p53 Tumor Suppressor. *PLoS Biol.* **2008**, *6*, e301. [CrossRef]
18. De Almeida, L.G.N.; Thode, H.; Eslambolchi, Y.; Chopra, S.; Young, D.; Gill, S.; Devel, L.; Dufour, A. Matrix Metalloproteinases: From Molecular Mechanisms to Physiology, Pathophysiology, and Pharmacology. *Pharmacol. Rev.* **2022**, *74*, 714–770. [CrossRef]
19. Park, J.-Y.; Choi, Y.; Kim, H.-D.; Kuo, H.-H.; Chang, Y.-C.; Kim, C.-H. Matrix Metalloproteinases and Their Inhibitors in the Pathogenesis of Epithelial Differentiation, Vascular Disease, Endometriosis, and Ocular Fibrotic Pterygium. *Int. J. Mol. Sci.* **2025**, *26*, 5553. [CrossRef]
20. Niedernhofer, L.J.; Robbins, P.D. Senotherapeutics for healthy ageing. *Nat. Rev. Drug Discov.* **2018**, *17*, 377. [CrossRef]
21. Rammah, M.; Dandachi, F.; Salman, R.; Shihadeh, A.; El-Sabban, M. In vitro effects of waterpipe smoke condensate on endothelial cell function: A potential risk factor for vascular disease. *Toxicol. Lett.* **2013**, *219*, 133–142. [CrossRef] [PubMed]
22. Giebe, S.; Cockcroft, N.; Hewitt, K.; Brux, M.; Hofmann, A.; Morawietz, H.; Brunssen, C. Cigarette smoke extract counteracts atheroprotective effects of high laminar flow on endothelial function. *Redox Biol.* **2017**, *12*, 776–786. [CrossRef] [PubMed]

23. Su, L.; Zhao, M.; Ma, F.; An, Z.; Yue, Q.; Zhao, C.; Sun, X.; Zhang, S.; Xu, J.; Jiang, X.; et al. A comparative assessment of e-cigarette aerosol extracts and tobacco cigarette smoke extracts on in vitro endothelial cell inflammation response. *Hum. Exp. Toxicol.* **2022**, *41*, 09603271221088996. [CrossRef]
24. Liang, G.; He, Z.; Peng, H.; Zeng, M.; Zhang, X. Cigarette smoke extract induces the senescence of endothelial progenitor cells by upregulating p300. *Tob. Induc. Dis.* **2023**, *21*, 122. [CrossRef]
25. Saxton, R.A.; Sabatini, D.M. mTOR Signaling in Growth, Metabolism, and Disease. *Cell* **2017**, *168*, 960–976. Erratum in *Cell* **2017**, *169*, 361–371. https://doi.org/10.1016/j.cell.2017.03.035. [CrossRef]
26. Mossmann, D.; Park, S.; Hall, M.N. mTOR signalling and cellular metabolism are mutual determinants in cancer. *Nat. Rev. Cancer* **2018**, *18*, 744–757. [CrossRef]
27. Mason, E.C.; Menon, S.; Schneider, B.R.; Gaskill, C.F.; Dawson, M.M.; Moore, C.M.; Armstrong, L.C.; Cho, O.; Richmond, B.W.; Kropski, J.A.; et al. Activation of mTOR signaling in adult lung microvascular progenitor cells accelerates lung aging. *J. Clin. Investig.* **2023**, *133*, e171430. [CrossRef]
28. Harrison, D.E.; Strong, R.; Sharp, Z.D.; Nelson, J.F.; Astle, C.M.; Flurkey, K.; Nadon, N.L.; Wilkinson, J.E.; Frenkel, K.; Carter, C.S.; et al. Rapamycin fed late in life extends lifespan in genetically heterogeneous mice. *Nature* **2009**, *460*, 392–395. [CrossRef]
29. Rodrik-Outmezguine, V.S.; Okaniwa, M.; Yao, Z.; Novotny, C.J.; McWhirter, C.; Banaji, A.; Won, H.; Wong, W.; Berger, M.; De Stanchina, E.; et al. Overcoming mTOR resistance mutations with a new-generation mTOR inhibitor. *Nature* **2016**, *534*, 272–276. [CrossRef]
30. Picos, A.; Seoane, N.; Campos-Toimil, M.; Viña, D. Vascular senescence and aging: Mechanisms, clinical implications, and therapeutic prospects. *Biogerontology* **2025**, *26*, 118. [CrossRef] [PubMed]
31. Zhou, H.; Li, X.; Rana, M.; Cornelius, J.F.; Khan, D.; Muhammad, S. mTOR Inhibitor Rapalink-1 Prevents Ethanol-Induced Senescence in Endothelial Cells. *Cells* **2023**, *12*, 2609. [CrossRef]
32. Ungvari, Z.; Tarantini, S.; Donato, A.J.; Galvan, V.; Csiszar, A. Mechanisms of Vascular Aging. *Circ. Res.* **2018**, *123*, 849–867. [CrossRef] [PubMed]
33. Herranz, N.; Gil, J. Mechanisms and functions of cellular senescence. *J. Clin. Investig.* **2018**, *128*, 1238–1246. [CrossRef]
34. Seo, Y.-S.; Park, J.-M.; Kim, J.-H.; Lee, M.-Y. Cigarette Smoke-Induced Reactive Oxygen Species Formation: A Concise Review. *Antioxidants* **2023**, *12*, 1732. [CrossRef]
35. Childs, B.G.; Durik, M.; Baker, D.J.; Van Deursen, J.M. Cellular senescence in aging and age-related disease: From mechanisms to therapy. *Nat. Med.* **2015**, *21*, 1424–1435. [CrossRef] [PubMed]
36. Gorgoulis, V.; Adams, P.D.; Alimonti, A.; Bennett, D.C.; Bischof, O.; Bishop, C.; Campisi, J.; Collado, M.; Evangelou, K.; Ferbeyre, G.; et al. Cellular Senescence: Defining a Path Forward. *Cell* **2019**, *179*, 813–827. [CrossRef]
37. Glorieux, C.; Enríquez, C.; Buc Calderon, P. The complex interplay between redox dysregulation and mTOR signaling pathway in cancer: A rationale for cancer treatment. *Biochem. Pharmacol.* **2025**, *232*, 116729. [CrossRef]
38. Visse, R.; Nagase, H. Matrix Metalloproteinases and Tissue Inhibitors of Metalloproteinases: Structure, Function, and Biochemistry. *Circ. Res.* **2003**, *92*, 827–839. [CrossRef]
39. Atkinson, G.; Bianco, R.; Di Gregoli, K.; Johnson, J.L. The contribution of matrix metalloproteinases and their inhibitors to the development, progression, and rupture of abdominal aortic aneurysms. *Front. Cardiovasc. Med.* **2023**, *10*, 1248561. [CrossRef] [PubMed]
40. Yanagisawa, H.; Davis, E.C.; Starcher, B.C.; Ouchi, T.; Yanagisawa, M.; Richardson, J.A.; Olson, E.N. Fibulin-5 is an elastin-binding protein essential for elastic fibre development in vivo. *Nature* **2002**, *415*, 168–171. [CrossRef]
41. Kim, Y.C.; Guan, K.-L. mTOR: A pharmacologic target for autophagy regulation. *J. Clin. Investig.* **2015**, *125*, 25–32. [CrossRef] [PubMed]
42. Anerillas, C.; Altés, G.; Gorospe, M. MAPKs in the early steps of senescence implementation. *Front. Cell Dev. Biol.* **2023**, *11*, 1083401. [CrossRef]
43. Ya, J.; Bayraktutan, U. Senolytics and Senomorphics Targeting p38MAPK/NF-κB Pathway Protect Endothelial Cells from Oxidative Stress-Mediated Premature Senescence. *Cells* **2024**, *13*, 1292. [CrossRef] [PubMed]
44. Zhang, C.; Qin, S.; Qin, L.; Liu, L.; Sun, W.; Li, X.; Li, N.; Wu, R.; Wang, X. Cigarette smoke extract-induced p120-mediated NF-κB activation in human epithelial cells. *Sci. Rep.* **2016**, *6*, 23131. [CrossRef] [PubMed]
45. Han, Z.; Wang, K.; Ding, S.; Zhang, M. Cross-talk of inflammation and cellular senescence. *Bone Res.* **2024**, *12*, 69. [CrossRef]
46. Yoshida, T.; Mett, I.; Bhunia, A.K.; Bowman, J.; Perez, M.; Zhang, L.; Gandjeva, A.; Zhen, L.; Chukwueke, U.; Mao, T.; et al. Rtp801, a suppressor of mTOR signaling, is an essential mediator of cigarette smoke-induced pulmonary injury and emphysema. *Nat. Med.* **2010**, *16*, 767–773. [CrossRef]
47. Laplante, M.; Sabatini, D.M. Regulation of mTORC1 and its impact on gene expression at a glance. *J. Cell Sci.* **2013**, *126*, 1713–1719. [CrossRef]
48. Liu, G.Y.; Sabatini, D.M. mTOR at the nexus of nutrition, growth, ageing and disease. *Nat. Rev. Mol. Cell Biol.* **2020**, *21*, 183–203. Erratum in *Nat. Rev. Mol. Cell Biol.* **2020**, *21*, 246. https://doi.org/10.1038/s41580-020-0219-y. [CrossRef]

49. Xue, J.; Liao, Q.; Luo, M.; Hua, C.; Zhao, J.; Yu, G.; Chen, X.; Li, X.; Zhang, X.; Ran, R.; et al. Cigarette smoke-induced oxidative stress activates NRF2 to mediate fibronectin disorganization in vascular formation. *Open Biol.* **2022**, *12*, 210310. [CrossRef]
50. Chandrasekaran, A.; Idelchik, M.D.P.S.; Melendez, J.A. Redox control of senescence and age-related disease. *Redox Biol.* **2017**, *11*, 91–102. [CrossRef]
51. Messner, B.; Bernhard, D. Smoking and Cardiovascular Disease: Mechanisms of Endothelial Dysfunction and Early Atherogenesis. *Arterioscler. Thromb. Vasc. Biol.* **2014**, *34*, 509–515. [CrossRef] [PubMed]
52. Pervin, M.; De Haan, J.B. Dysregulated Redox Signaling and Its Impact on Inflammatory Pathways, Mitochondrial Dysfunction, Autophagy and Cardiovascular Diseases. *Antioxidants* **2025**, *14*, 1278. [CrossRef] [PubMed]

3. Discussion

The present thesis investigated whether SC induces stress- and senescence-associated changes in vascular cells and whether these changes are attenuated by Rapalink-1. The results show that SC increased oxidative stress-related readouts, DNA damage markers, senescence-associated changes, inflammatory and ECM-related transcriptional responses, and phosphorylation-related signaling outputs in HUVECs and SMCs. Rapalink-1 reduced several of these responses, supporting the interpretation that dual mTORC1/2 inhibition affects key components of the SC-induced vascular stress response [105].

SC induced oxidative and genotoxic stress in both vascular cell types. This finding is consistent with the known ability of tobacco smoke constituents to disturb redox homeostasis and promote oxidative damage [19,20,36,37]. In vascular cells, endogenous ROS-generating systems such as NADPH oxidases may further increase the initial oxidative burden, and NADPH oxidase-related signaling has been implicated in vascular oxidative stress and cardiovascular disease [106,107]. At the same time, redox-responsive protective pathways, including the NRF2-regulated antioxidant response, may be activated as part of the cellular adaptation to oxidative injury [108]. Mitochondrial ROS generation may also contribute when cellular homeostasis is disturbed [109]. Thus, SC-induced oxidative stress should be interpreted as a dynamic response involving both damaging and compensatory processes.

In the present model, increased oxidation-sensitive fluorescence was accompanied by DNA damage-associated readouts, including γ-H2AX and 8-OHDG. This combination is relevant because oxidative stress alone is a broad and relatively non-specific cellular response, whereas the parallel detection of DNA damage markers indicates downstream genotoxic injury. Rapalink-1 reduced these oxidative stress- and DNA damage-associated readouts. However, this finding should not be interpreted as evidence that Rapalink-1 acts as a direct antioxidant. DCFH-DA-based measurements provide an overall oxidation-sensitive signal but do not identify a specific ROS species or its subcellular origin [55–57]. The effect of Rapalink-1 is therefore more appropriately interpreted as attenuation of oxidative stress-associated cellular responses rather than direct ROS scavenging.

SC also induced several senescence-associated changes, including increased SA-β-gal activity, reduced Lamin B1 expression, increased p21 expression, and accumulation of

DNA damage markers. This marker combination is important because cellular senescence is heterogeneous and cannot be reliably defined by a single readout alone [13–15,44,45]. Senescence can have context-dependent effects. In some settings, it may contribute to tissue repair and damage limitation, whereas persistent accumulation of senescent cells can promote chronic dysfunction through inflammatory and remodeling-related mechanisms [110]. In vascular cells, this distinction is relevant because senescence of both endothelial cells and SMCs may affect vessel wall homeostasis.

The response pattern differed between HUVECs and SMCs. In HUVECs, SC induced a clearer SA-β-gal response together with molecular senescence markers. In SMCs, the phenotype was more strongly supported by Lamin B1 reduction, p21 induction, and DNA damage-associated changes. This difference is biologically plausible because senescence marker expression depends on cell type, stress intensity, exposure duration, and cellular context. Endothelial aging and senescence have been linked to impaired vascular homeostasis, reduced protective endothelial functions, and pro-inflammatory activation [111]. In contrast, SMC senescence may contribute to altered phenotypic stability, ECM remodeling, and plaque vulnerability [112,113]. These differences support the inclusion of both vascular cell types in the present study.

Another finding is that SC induced SASP-associated inflammatory responses. The SASP is not a fixed program but a variable secretory phenotype shaped by cell type, stress stimulus, and signaling context [63–67]. It includes cytokines, chemokines, growth factors, adhesion molecules, and proteases that can affect neighboring cells and modify the extracellular environment [114,115]. Upstream inflammatory regulators, including IL-1α-associated signaling, can contribute to SASP amplification [116]. In this study, SC increased inflammatory and matrix-related transcripts in vascular cells, suggesting that tobacco-derived stress promotes not only intracellular injury but also secretory and remodeling responses.

The ECM-related findings are particularly relevant for the vascular interpretation of this work. The vascular ECM provides mechanical support, regulates vessel wall elasticity, and influences vascular cell behavior [117]. MMPs and TIMPs are important regulators of ECM turnover and have been implicated in vascular remodeling and atherogenesis [118,119]. Elastic fiber-associated proteins, including fibulin family members, are also important for vessel wall integrity and elastic fiber organization [120,121]. In the present study, SC altered MMP-related responses and reduced ECM-associated transcripts such as ELN, COL1A1, and EFEMP1 in SMCs. These findings

suggest that SC-induced senescence-associated changes may contribute to maladaptive vascular remodeling.

At the signaling level, the present data implicate NF-κB-, MAPK-, and mTOR-related pathways as components of the SC response. NF-κB and MAPK signaling can link oxidative stress to inflammatory gene expression, whereas mTOR signaling integrates growth, metabolism, protein synthesis, autophagy, and stress adaptation [71–96]. mTOR has also been connected to the regulation of senescence-associated inflammatory output. Experimental studies have shown that mTOR can influence SASP regulation through translational and stress-response mechanisms [122,123]. Mitochondrial dysfunction may further shape senescence-associated secretory profiles, indicating that metabolic and inflammatory remodeling are closely connected during senescence [124].

Rapalink-1 reduced several phosphorylation-related signaling readouts, including p65-, p38-, ERK-, S6-, and AKT-associated changes. This supports the interpretation that Rapalink-1 affects several signaling components rather than a single terminal endpoint. Nevertheless, these findings should be interpreted with caution. The present study does not establish a direct causal hierarchy among oxidative stress, NF-κB activation, MAPK signaling, mTOR-related pathway output, and senescence-associated remodeling. Broader mTOR inhibitors were developed to overcome limitations of rapamycin-sensitive pathway inhibition, but their cellular effects may still depend on context, dose, exposure time, and compensatory signaling [94–100,125].

From a translational perspective, the present findings support the view that SC-induced vascular injury involves oxidative, inflammatory, senescence-associated, and matrix-remodeling processes. Clinical evidence has shown that anti-inflammatory intervention can reduce cardiovascular events in selected patient populations, highlighting the relevance of inflammation as a therapeutic target in cardiovascular disease [126]. However, based on the present in vitro data, Rapalink-1 should not be interpreted as a clinically applicable vascular therapy. Rather, it should be viewed as an experimental tool to examine how mTOR-related signaling contributes to SC-induced vascular cell stress.

The broader senescence literature also supports the view that senescence is a modifiable process. Genetic and pharmacological studies have shown that reducing the burden of senescent cells can delay or improve several age-associated phenotypes in experimental systems [127,128]. These findings have generated interest in senotherapeutic

approaches, although translation to human vascular disease remains challenging and requires careful evaluation of safety, specificity, timing, and tissue context [129,130]. The present work does not test senolytic therapy or senescent cell clearance. Instead, it suggests that modulation of senescence-associated signaling by Rapalink-1 may reduce the development of an SC-induced senescence-like phenotype in vascular cells.

One major limitation of the present study is that it was conducted in vitro. Cultured HUVECs and SMCs allow controlled mechanistic investigation, but this model cannot reproduce the full complexity of smoking-related vascular disease in vivo. Chronic exposure, immune cell recruitment, platelet activation, circulating metabolites, hemodynamic forces, and tissue architecture are absent from the present model. In addition, although multiple markers were used to support the interpretation of senescence, the study does not directly demonstrate irreversible growth arrest, long-term persistence, or functional recovery after withdrawal of SC or Rapalink-1. Further work using pathway-specific inhibition, genetic approaches, rescue experiments, and disease-relevant in vivo models will be required to define the causal contribution of mTORC1, mTORC2, NF-κB, MAPK, and oxidative stress to the effects observed here.

Taken together, the data support a model in which SC induces vascular cell injury involving oxidative stress, DNA damage, senescence-associated marker changes, SASP-related inflammation, ECM remodeling, and activation of stress-responsive signaling. Rapalink-1 reduced several components of this response, suggesting that mTORC1/2 inhibition can affect key stress- and senescence-associated processes in smoke-exposed vascular cells. These findings provide a basis for further investigation of mTOR-related signaling in smoking-associated vascular aging and remodeling.

3.1. Limitations

Several limitations should be acknowledged. First, the experiments were performed in vitro using cultured HUVECs and SMCs. This model allows controlled analysis of vascular cell stress responses but cannot reproduce the structural, mechanical, metabolic, and immunological complexity of the vascular wall in vivo. Second, the model does not include interactions with immune cells, fibroblasts, platelets, circulating factors, or hemodynamic forces, all of which may influence smoking-related vascular injury.

Third, the present work focused on short-term SC exposure and early senescence-associated responses. It therefore does not address long-term persistence, reversibility,

or chronic adaptation after smoke-derived injury. Fourth, although the data support changes in NF-κB-, MAPK-, and downstream mTOR-related signaling after Rapalink-1 treatment, the study does not establish a direct causal hierarchy among these pathways. It also does not determine whether all observed effects are directly mTOR-dependent or partly mediated by secondary changes in the cellular stress response.

Finally, although Rapalink-1 attenuated several stress-associated responses in vitro, these findings do not establish clinical relevance or therapeutic applicability. Future studies using chronic smoke exposure models, pathway-specific interventions, genetic approaches, and disease-relevant in vivo systems will be required to validate these findings and to define the safety and mechanistic scope of dual mTORC1/2 inhibition in vascular aging.

3.2. Conclusion

In conclusion, the present study shows that SC induces oxidative stress, DNA damage, senescence-associated changes, inflammatory activation, and ECM-related alterations in HUVECs and SMCs. Dual mTORC1/2 inhibition with Rapalink-1 attenuated several of these responses, including oxidative and genotoxic injury, senescence-associated markers, selected SASP-related transcriptional changes, and downstream inflammatory and mTOR-related signaling readouts.

These findings indicate that Rapalink-1 affects key components of the SC-induced vascular stress response in vitro. They also support further investigation of mTOR-related signaling as a regulatory pathway in smoking-related vascular aging and remodeling.

4. References

1. Ambrose JA, Barua RS. The pathophysiology of cigarette smoking and cardiovascular disease: an update. J Am Coll Cardiol. 2004;43(10):1731–1737. doi:10.1016/j.jacc.2003.12.047.

2. Messner B, Bernhard D. Smoking and cardiovascular disease: mechanisms of endothelial dysfunction and early atherogenesis. Arterioscler Thromb Vasc Biol. 2014;34(3):509–515. doi:10.1161/ATVBAHA.113.300156.

3. Morris PB, Ference BA, Jahangir E, Feldman DN, Ryan JJ, Bahrami H, et al. Cardiovascular effects of exposure to cigarette smoke and electronic cigarettes. J Am Coll Cardiol. 2015;66(12):1378–1391. doi:10.1016/j.jacc.2015.07.037.

4. Benowitz NL, Burbank AD. Cardiovascular toxicity of nicotine: implications for electronic cigarette use. Trends Cardiovasc Med. 2016;26(6):515–523. doi:10.1016/j.tcm.2016.03.001.

5. Shah RS, Cole JW. Smoking and stroke: the more you smoke the more you stroke. Expert Rev Cardiovasc Ther. 2010;8(7):917–932. doi:10.1586/erc.10.56.

6. Etminan N, Rinkel GJE. Unruptured intracranial aneurysms: development, rupture and preventive management. Nat Rev Neurol. 2016;12(12):699–713. doi:10.1038/nrneurol.2016.150.

7. Wang H, Wang L, Wang J, Zhang L, Li C. The biological effects of smoking on the formation and rupture of intracranial aneurysms: a systematic review and meta-analysis. Front Neurol. 2022;13:862916. doi:10.3389/fneur.2022.862916.

8. Sturtzel C. Endothelial cells. Adv Exp Med Biol. 2017;1003:71–91. doi:10.1007/978-3-319-57613-8_4.

9. Pearson JD. Endothelial cell function and thrombosis. Baillieres Best Pract Res Clin Haematol. 1999;12(3):329–341. doi:10.1053/beha.1999.0028.

10. Gimbrone MA Jr, García-Cardeña G. Endothelial cell dysfunction and the pathobiology of atherosclerosis. Circ Res. 2016;118(4):620–636. doi:10.1161/CIRCRESAHA.115.306301.

11. Owens GK, Kumar MS, Wamhoff BR. Molecular regulation of vascular smooth muscle cell differentiation in development and disease. Physiol Rev. 2004;84(3):767–801. doi:10.1152/physrev.00041.2003.

12. Bennett MR, Sinha S, Owens GK. Vascular smooth muscle cells in atherosclerosis.

Circ Res. 2016;118(4):692–702. doi:10.1161/CIRCRESAHA.115.306361.

13. Gorgoulis V, Adams PD, Alimonti A, Bennett DC, Bischof O, Bishop C, et al. Cellular senescence: defining a path forward. Cell. 2019;179(4):813–827. doi:10.1016/j.cell.2019.10.005.

14. Herranz N, Gil J. Mechanisms and functions of cellular senescence. J Clin Invest. 2018;128(4):1238–1246. doi:10.1172/JCI95148.

15. Childs BG, Durik M, Baker DJ, Van Deursen JM. Cellular senescence in aging and age-related disease: from mechanisms to therapy. Nat Med. 2015;21(12):1424–1435. doi:10.1038/nm.4000.

16. Ungvari Z, Tarantini S, Donato AJ, Galvan V, Csiszar A. Mechanisms of vascular aging. Circ Res. 2018;123(7):849–867. doi:10.1161/CIRCRESAHA.118.311378.

17. Katsuumi G, Shimizu I, Yoshida Y, Minamino T. Vascular senescence in cardiovascular and metabolic diseases. Front Cardiovasc Med. 2018;5:18. doi:10.3389/fcvm.2018.00018.

18. Owens WA, Walaszczyk A, Spyridopoulos I, Dookun E, Richardson GD. Senescence and senolytics in cardiovascular disease: promise and potential pitfalls. Mech Ageing Dev. 2021;198:111540. doi:10.1016/j.mad.2021.111540.

19. Talhout R, Schulz T, Florek E, Van Benthem J, Wester P, Opperhuizen A. Hazardous compounds in tobacco smoke. Int J Environ Res Public Health. 2011;8(2):613–628. doi:10.3390/ijerph8020613.

20. Valavanidis A, Vlachogianni T, Fiotakis K. Tobacco smoke: involvement of reactive oxygen species and stable free radicals in mechanisms of oxidative damage, carcinogenesis and synergistic effects with other respirable particles. Int J Environ Res Public Health. 2009;6(2):445–462. doi:10.3390/ijerph6020445.

21. Hecht SS. Tobacco carcinogens, their biomarkers and tobacco-induced cancer. Nat Rev Cancer. 2003;3(10):733–744. doi:10.1038/nrc1190.

22. Rammah M, Dandachi F, Salman R, Shihadeh A, El-Sabban M. In vitro effects of waterpipe smoke condensate on endothelial cell function: a potential risk factor for vascular disease. Toxicol Lett. 2013;219(2):133–142. doi:10.1016/j.toxlet.2013.02.015.

23. Giebe S, Cockcroft N, Hewitt K, Brux M, Hofmann A, Morawietz H, et al. Cigarette smoke extract counteracts atheroprotective effects of high laminar flow on endothelial function. Redox Biol. 2017;12:776–786. doi:10.1016/j.redox.2017.04.008.

24. Su L, Zhao M, Ma F, An Z, Yue Q, Zhao C, et al. A comparative assessment of e-

cigarette aerosol extracts and tobacco cigarette smoke extracts on in vitro endothelial cell inflammation response. Hum Exp Toxicol. 2022;41:09603271221088996. doi:10.1177/09603271221088996.

25. Barbieri SS, Zacchi E, Amadio P, Gianellini S, Mussoni L, Weksler BB, et al. Cytokines present in smokers' serum interact with smoke components to enhance endothelial dysfunction. Cardiovasc Res. 2011;90(3):475–483. doi:10.1093/cvr/cvr032.

26. Deanfield JE, Halcox JP, Rabelink TJ. Endothelial function and dysfunction: testing and clinical relevance. Circulation. 2007;115(10):1285–1295. doi:10.1161/CIRCULATIONAHA.106.652859.

27. Pober JS, Sessa WC. Evolving functions of endothelial cells in inflammation. Nat Rev Immunol. 2007;7(10):803–815. doi:10.1038/nri2171.

28. Aird WC. Phenotypic heterogeneity of the endothelium: I. Structure, function, and mechanisms. Circ Res. 2007;100(2):158–173. doi:10.1161/01.RES.0000255691.76142.4a.

29. Yau JW, Teoh H, Verma S. Endothelial cell control of thrombosis. BMC Cardiovasc Disord. 2015;15:130. doi:10.1186/s12872-015-0124-z.

30. Onat D, Brillon D, Colombo PC, Schmidt AM. Human vascular endothelial cells: a model system for studying vascular inflammation in diabetes and atherosclerosis. Curr Diab Rep. 2011;11(3):193–202. doi:10.1007/s11892-011-0182-2.

31. Ross R. Atherosclerosis—an inflammatory disease. N Engl J Med. 1999;340(2):115–126. doi:10.1056/NEJM199901143400207.

32. Libby P. Inflammation in atherosclerosis. Nature. 2002;420(6917):868–874. doi:10.1038/nature01323.

33. Bierhansl L, Conradi LC, Treps L, Dewerchin M, Carmeliet P. Central role of metabolism in endothelial cell function and vascular disease. Physiology (Bethesda). 2017;32(2):126–140. doi:10.1152/physiol.00031.2016.

34. Medina-Leyte DJ, Zepeda-Garcia O, Dominguez-Perez M, Gonzalez-Garrido A, Villarreal-Molina T, Jacobo-Albavera L. Endothelial dysfunction, inflammation and coronary artery disease: potential biomarkers and promising therapeutical approaches. Int J Mol Sci. 2021;22(8):3850. doi:10.3390/ijms22083850.

35. Lusis AJ. Atherosclerosis. Nature. 2000;407(6801):233–241. doi:10.1038/35025203.

36. Sies H. Oxidative stress: a concept in redox biology and medicine. Redox Biol.

2015;4:180–183. doi:10.1016/j.redox.2015.01.002.

37. Liguori I, Russo G, Curcio F, Bulli G, Aran L, Della-Morte D, et al. Oxidative stress, aging, and diseases. Clin Interv Aging. 2018;13:757–772. doi:10.2147/CIA.S158513.

38. Stocker R, Keaney JF Jr. Role of oxidative modifications in atherosclerosis. Physiol Rev. 2004;84(4):1381–1478. doi:10.1152/physrev.00047.2003.

39. Förstermann U, Sessa WC. Nitric oxide synthases: regulation and function. Eur Heart J. 2012;33(7):829–837. doi:10.1093/eurheartj/ehr304.

40. Cadet J, Davies KJA. Oxidative DNA damage and repair: an introduction. Free Radic Biol Med. 2017;107:2–12. doi:10.1016/j.freeradbiomed.2017.03.030.

41. Cooke MS, Evans MD, Dizdaroglu M, Lunec J. Oxidative DNA damage: mechanisms, mutation, and disease. FASEB J. 2003;17(10):1195–1214. doi:10.1096/fj.02-0752rev.

42. d'Adda di Fagagna F, Reaper PM, Clay-Farrace L, Fiegler H, Carr P, Von Zglinicki T, et al. A DNA damage checkpoint response in telomere-initiated senescence. Nature. 2003;426(6963):194–198. doi:10.1038/nature02118.

43. Rodier F, Coppé JP, Patil CK, Hoeijmakers WA, Muñoz DP, Raza SR, et al. Persistent DNA damage signalling triggers senescence-associated inflammatory cytokine secretion. Nat Cell Biol. 2009;11(8):973–979. doi:10.1038/ncb1909.

44. Hernandez-Segura A, Nehme J, Demaria M. Hallmarks of cellular senescence. Trends Cell Biol. 2018;28(6):436–453. doi:10.1016/j.tcb.2018.02.001.

45. Sharpless NE, Sherr CJ. Forging a signature of in vivo senescence. Nat Rev Cancer. 2015;15(7):397–408. doi:10.1038/nrc3960.

46. Dimri GP, Lee X, Basile G, Acosta M, Scott G, Roskelley C, et al. A biomarker that identifies senescent human cells in culture and in aging skin in vivo. Proc Natl Acad Sci U S A. 1995;92(20):9363–9367. doi:10.1073/pnas.92.20.9363.

47. Lee BY, Han JA, Im JS, Morrone A, Johung K, Goodwin EC, et al. Senescence-associated beta-galactosidase is lysosomal beta-galactosidase. Aging Cell. 2006;5(2):187–195. doi:10.1111/j.1474-9726.2006.00199.x.

48. Itahana K, Campisi J, Dimri GP. Methods to detect biomarkers of cellular senescence: the senescence-associated beta-galactosidase assay. Methods Mol Biol. 2007;371:21–31. doi:10.1007/978-1-59745-361-5_3.

49. Yang NC, Hu ML. The limitations and validities of senescence-associated beta-

galactosidase activity as an aging marker for human foreskin fibroblast Hs68 cells. Exp Gerontol. 2005;40(10):813–819. doi:10.1016/j.exger.2005.07.011.

50. Freund A, Laberge RM, Demaria M, Campisi J. Lamin B1 loss is a senescence-associated biomarker. Mol Biol Cell. 2012;23(11):2066–2075. doi:10.1091/mbc.E11-10-0884.

51. Shimi T, Butin-Israeli V, Adam SA, Hamanaka RB, Goldman AE, Lucas CA, et al. The role of nuclear lamin B1 in cell proliferation and senescence. Genes Dev. 2011;25(24):2579–2593. doi:10.1101/gad.179515.111.

52. Karimian A, Ahmadi Y, Yousefi B. Multiple functions of p21 in cell cycle, apoptosis and transcriptional regulation after DNA damage. DNA Repair (Amst). 2016;42:63–71. doi:10.1016/j.dnarep.2016.04.008.

53. Gartel AL, Serfas MS, Tyner AL. p21--negative regulator of the cell cycle. Proc Soc Exp Biol Med. 1996;213(2):138–149. doi:10.3181/00379727-213-44046.

54. Baus F, Gire V, Fisher D, Piette J, Dulić V. Permanent cell cycle exit in G2 phase after DNA damage in normal human fibroblasts. EMBO J. 2003;22(15):3992–4002. doi:10.1093/emboj/cdg387.

55. Kalyanaraman B, Darley-Usmar V, Davies KJA, Dennery PA, Forman HJ, Grisham MB, et al. Measuring reactive oxygen and nitrogen species with fluorescent probes: challenges and limitations. Free Radic Biol Med. 2012;52(1):1–6. doi:10.1016/j.freeradbiomed.2011.09.030.

56. Eruslanov E, Kusmartsev S. Identification of ROS using oxidized DCFDA and flow-cytometry. Methods Mol Biol. 2010;594:57–72. doi:10.1007/978-1-60761-411-1_4.

57. Winterbourn CC. The challenges of using fluorescent probes to detect and quantify specific reactive oxygen species in living cells. Biochim Biophys Acta. 2014;1840(2):730–738. doi:10.1016/j.bbagen.2013.05.004.

58. Rogakou EP, Pilch DR, Orr AH, Ivanova VS, Bonner WM. DNA double-stranded breaks induce histone H2AX phosphorylation on serine 139. J Biol Chem. 1998;273(10):5858–5868. doi:10.1074/jbc.273.10.5858.

59. Mah LJ, El-Osta A, Karagiannis TC. γH2AX: a sensitive molecular marker of DNA damage and repair. Leukemia. 2010;24(4):679–686. doi:10.1038/leu.2010.6.

60. Kasai H, Hayami H, Yamaizumi Z, Saito H, Nishimura S. Detection and identification of mutagens and carcinogens as their adducts with guanosine derivatives.

Nucleic Acids Res. 1984;12(4):2127–2136. doi:10.1093/nar/12.4.2127.

61. Valavanidis A, Vlachogianni T, Fiotakis C. 8-hydroxy-2′-deoxyguanosine (8-OHdG): a critical biomarker of oxidative stress and carcinogenesis. J Environ Sci Health C Environ Carcinog Ecotoxicol Rev. 2009;27(2):120–139. doi:10.1080/10590500902885684.

62. Pilger A, Rüdiger HW. 8-Hydroxy-2′-deoxyguanosine as a marker of oxidative DNA damage related to occupational and environmental exposures. Int Arch Occup Environ Health. 2006;80(1):1–15. doi:10.1007/s00420-006-0106-7.

63. Kuilman T, Michaloglou C, Mooi WJ, Peeper DS. The essence of senescence. Genes Dev. 2010;24(22):2463–2479. doi:10.1101/gad.1971610.

64. Coppé JP, Patil CK, Rodier F, Sun Y, Muñoz DP, Goldstein J, et al. Senescence-associated secretory phenotypes reveal cell-nonautonomous functions of oncogenic RAS and the p53 tumor suppressor. PLoS Biol. 2008;6(12):e301. doi:10.1371/journal.pbio.0060301.

65. Acosta JC, Banito A, Wuestefeld T, Georgilis A, Janich P, Morton JP, et al. A complex secretory program orchestrated by the inflammasome controls paracrine senescence. Nat Cell Biol. 2013;15(8):978–990. doi:10.1038/ncb2784.

66. van Deursen JM. The role of senescent cells in ageing. Nature. 2014;509(7501):439–446. doi:10.1038/nature13193.

67. Sun Y, Wang X, Liu T, Zhu X, Pan X. The multifaceted role of the SASP in atherosclerosis: from mechanisms to therapeutic opportunities. Cell Biosci. 2022;12(1):74. doi:10.1186/s13578-022-00815-5.

68. De Almeida LGN, Thode H, Eslambolchi Y, Chopra S, Young D, Gill S, et al. Matrix metalloproteinases: from molecular mechanisms to physiology, pathophysiology, and pharmacology. Pharmacol Rev. 2022;74(3):714–770. doi:10.1124/pharmrev.121.000349.

69. Visse R, Nagase H. Matrix metalloproteinases and tissue inhibitors of metalloproteinases: structure, function, and biochemistry. Circ Res. 2003;92(8):827–839. doi:10.1161/01.RES.0000070112.80711.3D.

70. Cabral-Pacheco GA, Garza-Veloz I, Castruita-De la Rosa C, Ramirez-Acuña JM, Perez-Romero BA, Guerrero-Rodriguez JF, et al. The roles of matrix metalloproteinases and their inhibitors in human diseases. Int J Mol Sci. 2020;21(24):9739. doi:10.3390/ijms21249739.

71. Karin M, Ben-Neriah Y. Phosphorylation meets ubiquitination: the control of NF-kappaB activity. Annu Rev Immunol. 2000;18:621–663. doi:10.1146/annurev.immunol.18.1.621.

72. Hayden MS, Ghosh S. NF-kappaB, the first quarter-century: remarkable progress and outstanding questions. Genes Dev. 2012;26(3):203–234. doi:10.1101/gad.183434.111.

73. Morgan MJ, Liu ZG. Crosstalk of reactive oxygen species and NF-kappaB signaling. Cell Res. 2011;21(1):103–115. doi:10.1038/cr.2010.178.

74. Lawrence T. The nuclear factor NF-kappaB pathway in inflammation. Cold Spring Harb Perspect Biol. 2009;1(6):a001651. doi:10.1101/cshperspect.a001651.

75. Salminen A, Kauppinen A, Kaarniranta K. Emerging role of NF-kappaB signaling in the induction of senescence-associated secretory phenotype. Cell Signal. 2012;24(4):835–845. doi:10.1016/j.cellsig.2011.12.006.

76. Rovillain E, Mansfield L, Caetano C, Alvarez-Fernandez M, Caballero OL, Medema RH, et al. Activation of nuclear factor-kappa B signalling promotes cellular senescence. Oncogene. 2011;30(20):2356–2366. doi:10.1038/onc.2010.611.

77. Widmann C, Gibson S, Jarpe MB, Johnson GL. Mitogen-activated protein kinase: conservation of a three-kinase module from yeast to human. Physiol Rev. 1999;79(1):143–180. doi:10.1152/physrev.1999.79.1.143.

78. Cargnello M, Roux PP. Activation and function of the MAPKs and their substrates, the MAPK-activated protein kinases. Microbiol Mol Biol Rev. 2011;75(1):50–83. doi:10.1128/MMBR.00031-10.

79. Cuenda A, Rousseau S. p38 MAP-kinases pathway regulation, function and role in human diseases. Biochim Biophys Acta. 2007;1773(8):1358–1375. doi:10.1016/j.bbamcr.2007.03.010.

80. Kyriakis JM, Avruch J. Mammalian MAPK signal transduction pathways activated by stress and inflammation: a 10-year update. Physiol Rev. 2012;92(2):689–737. doi:10.1152/physrev.00028.2011.

81. Freund A, Patil CK, Campisi J. p38MAPK is a novel DNA damage response-independent regulator of the senescence-associated secretory phenotype. EMBO J. 2011;30(8):1536–1548. doi:10.1038/emboj.2011.69.

82. Alimbetov D, Davis T, Brook AJ, Cox LS, Faragher RGA, Nurgozhin T, et al. Suppression of the senescence-associated secretory phenotype in human fibroblasts

using small molecule inhibitors of p38 MAP kinase and MK2. Biogerontology. 2016;17(2):305–315. doi:10.1007/s10522-015-9610-z.

83. Anerillas C, Abdelmohsen K, Gorospe M. Regulation of senescence traits by MAPKs. Geroscience. 2020;42(2):397–408. doi:10.1007/s11357-020-00183-3.

84. Saha RN, Jana M, Pahan K. MAPK p38 regulates transcriptional activity of NF-kappaB in primary human astrocytes via acetylation of p65. J Immunol. 2007;179(10):7101–7109. doi:10.4049/jimmunol.179.10.7101.

85. Saxton RA, Sabatini DM. mTOR signaling in growth, metabolism, and disease. Cell. 2017;168(6):960–976. doi:10.1016/j.cell.2017.02.004.

86. Liu GY, Sabatini DM. mTOR at the nexus of nutrition, growth, ageing and disease. Nat Rev Mol Cell Biol. 2020;21(4):183–203. doi:10.1038/s41580-019-0199-y.

87. Laplante M, Sabatini DM. mTOR signaling in growth control and disease. Cell. 2012;149(2):274–293. doi:10.1016/j.cell.2012.03.017.

88. Zoncu R, Efeyan A, Sabatini DM. mTOR: from growth signal integration to cancer, diabetes and ageing. Nat Rev Mol Cell Biol. 2011;12(1):21–35. doi:10.1038/nrm3025.

89. Kim YC, Guan KL. mTOR: a pharmacologic target for autophagy regulation. J Clin Invest. 2015;125(1):25–32. doi:10.1172/JCI73939.

90. Sarbassov DD, Guertin DA, Ali SM, Sabatini DM. Phosphorylation and regulation of Akt/PKB by the rictor-mTOR complex. Science. 2005;307(5712):1098–1101. doi:10.1126/science.1106148.

91. Sarbassov DD, Ali SM, Sengupta S, Sheen JH, Hsu PP, Bagley AF, et al. Prolonged rapamycin treatment inhibits mTORC2 assembly and Akt/PKB. Mol Cell. 2006;22(2):159–168. doi:10.1016/j.molcel.2006.03.029.

92. Harrison DE, Strong R, Sharp ZD, Nelson JF, Astle CM, Flurkey K, et al. Rapamycin fed late in life extends lifespan in genetically heterogeneous mice. Nature. 2009;460(7253):392–395. doi:10.1038/nature08221.

93. Yoshida T, Mett I, Bhunia AK, Bowman J, Perez M, Zhang L, et al. Rtp801, a suppressor of mTOR signaling, is an essential mediator of cigarette smoke-induced pulmonary injury and emphysema. Nat Med. 2010;16(7):767–773. doi:10.1038/nm.2157.

94. Rodrik-Outmezguine VS, Okaniwa M, Yao Z, Novotny CJ, McWhirter C, Banaji A, et al. Overcoming mTOR resistance mutations with a new-generation mTOR inhibitor. Nature. 2016;534(7606):272–276. doi:10.1038/nature17963.

95. Li J, Kim SG, Blenis J. Rapamycin: one drug, many effects. Cell Metab. 2014;19(3):373–379. doi:10.1016/j.cmet.2014.01.001.

96. Lamming DW, Ye L, Katajisto P, Goncalves MD, Saitoh M, Stevens DM, et al. Rapamycin-induced insulin resistance is mediated by mTORC2 loss and uncoupled from longevity. Science. 2012;335(6076):1638–1643. doi:10.1126/science.1215135.

97. Thoreen CC, Kang SA, Chang JW, Liu Q, Zhang J, Gao Y, et al. An ATP-competitive mammalian target of rapamycin inhibitor reveals rapamycin-resistant functions of mTORC1. J Biol Chem. 2009;284(12):8023–8032. doi:10.1074/jbc.M900301200.

98. Feldman ME, Apsel B, Uotila A, Loewith R, Knight ZA, Ruggero D, et al. Active-site inhibitors of mTOR target rapamycin-resistant outputs of mTORC1 and mTORC2. PLoS Biol. 2009;7(2):e38. doi:10.1371/journal.pbio.1000038.

99. Ma XM, Blenis J. Molecular mechanisms of mTOR-mediated translational control. Nat Rev Mol Cell Biol. 2009;10(5):307–318. doi:10.1038/nrm2672.

100. Hsieh AC, Liu Y, Edlind MP, Ingolia NT, Janes MR, Sher A, et al. The translational landscape of mTOR signalling steers cancer initiation and metastasis. Nature. 2012;485(7396):55–61. doi:10.1038/nature10912.

101. Mannick JB, Del Giudice G, Lattanzi M, Valiante NM, Praestgaard J, Huang B, et al. mTOR inhibition improves immune function in the elderly. Sci Transl Med. 2014;6(268):268ra179. doi:10.1126/scitranslmed.3009892.

102. Demidenko ZN, Zubova SG, Bukreeva EI, Pospelov VA, Pospelova TV, Blagosklonny MV. Rapamycin decelerates cellular senescence. Cell Cycle. 2009;8(12):1888–1895. doi:10.4161/cc.8.12.8606.

103. Leontieva OV, Demidenko ZN, Blagosklonny MV. Rapamycin reverses insulin resistance and hepatic steatosis in obese mice. Aging (Albany NY). 2014;6(12):1009–1018. doi:10.18632/aging.100704.

104. Zhou H, Li X, Rana M, Cornelius JF, Khan D, Muhammad S. mTOR inhibitor Rapalink-1 prevents ethanol-induced senescence in endothelial cells. Cells. 2023;12(22):2609. doi:10.3390/cells12222609.

105. You J, Liu H, Khan D, Muhereza R, Faust K, Muhammad S. Smoke Condensate-Induced Vascular Senescence and SASP Are Attenuated by Dual mTORC1/2 Inhibition with Rapalink-1. Int J Mol Sci. 2026;27(8):3636. doi:10.3390/ijms27083636.

106. Bedard K, Krause KH. The NOX family of ROS-generating NADPH oxidases:

physiology and pathophysiology. Physiol Rev. 2007;87(1):245–313. doi:10.1152/physrev.00044.2005.

107. Drummond GR, Selemidis S, Griendling KK, Sobey CG. Combating oxidative stress in vascular disease: NADPH oxidases as therapeutic targets. Nat Rev Drug Discov. 2011;10(6):453–471. doi:10.1038/nrd3403.

108. Ma Q. Role of Nrf2 in oxidative stress and toxicity. Annu Rev Pharmacol Toxicol. 2013;53:401–426. doi:10.1146/annurev-pharmtox-011112-140320.

109. Murphy MP. How mitochondria produce reactive oxygen species. Biochem J. 2009;417(1):1–13. doi:10.1042/BJ20081386.

110. Demaria M, Ohtani N, Youssef SA, Rodier F, Toussaint W, Mitchell JR, et al. An essential role for senescent cells in optimal wound healing through secretion of PDGF-AA. Dev Cell. 2014;31(6):722–733. doi:10.1016/j.devcel.2014.11.012.

111. Donato AJ, Morgan RG, Walker AE, Lesniewski LA. Cellular and molecular biology of aging endothelial cells. J Mol Cell Cardiol. 2015;89(Pt B):122–135. doi:10.1016/j.yjmcc.2015.01.021.

112. Wang J, Uryga AK, Reinhold J, Figg N, Baker L, Finigan A, et al. Vascular smooth muscle cell senescence promotes atherosclerosis and features of plaque vulnerability. Circulation. 2015;132(20):1909–1919. doi:10.1161/CIRCULATIONAHA.115.016457.

113. Grootaert MOJ, Moulis M, Roth L, Martinet W, Vindis C, Bennett MR, et al. Vascular smooth muscle cell death, autophagy and senescence in atherosclerosis. Cardiovasc Res. 2018;114(4):622–634. doi:10.1093/cvr/cvy007.

114. Coppé JP, Desprez PY, Krtolica A, Campisi J. The senescence-associated secretory phenotype: the dark side of tumor suppression. Annu Rev Pathol. 2010;5:99–118. doi:10.1146/annurev-pathol-121808-102144.

115. Freund A, Orjalo AV, Desprez PY, Campisi J. Inflammatory networks during cellular senescence: causes and consequences. Trends Mol Med. 2010;16(5):238–246. doi:10.1016/j.molmed.2010.03.003.

116. Orjalo AV, Bhaumik D, Gengler BK, Scott GK, Campisi J. Cell surface-bound IL-1α is an upstream regulator of the senescence-associated IL-6/IL-8 cytokine network. Proc Natl Acad Sci U S A. 2009;106(40):17031–17036. doi:10.1073/pnas.0905299106.

117. Wagenseil JE, Mecham RP. Vascular extracellular matrix and arterial mechanics. Physiol Rev. 2009;89(3):957–989. doi:10.1152/physrev.00041.2008.

118. Galis ZS, Khatri JJ. Matrix metalloproteinases in vascular remodeling and

atherogenesis: the good, the bad, and the ugly. Circ Res. 2002;90(3):251–262. doi:10.1161/hh0302.105345.

119. Nagase H, Woessner JF Jr. Matrix metalloproteinases. J Biol Chem. 1999;274(31):21491–21494. doi:10.1074/jbc.274.31.21491.

120. Yanagisawa H, Davis EC, Starcher BC, Ouchi T, Yanagisawa M, Richardson JA, et al. Fibulin-5 is an elastin-binding protein essential for elastic fibre development in vivo. Nature. 2002;415(6868):168–171. doi:10.1038/415168a.

121. Nakamura T, Lozano PR, Ikeda Y, Iwanaga Y, Hinek A, Minamisawa S, et al. Fibulin-5/DANCE is essential for elastogenesis in vivo. Nature. 2002;415(6868):171–175. doi:10.1038/415171a.

122. Laberge RM, Sun Y, Orjalo AV, Patil CK, Freund A, Zhou L, et al. mTOR regulates the pro-tumorigenic senescence-associated secretory phenotype by promoting IL1A translation. Nat Cell Biol. 2015;17(8):1049–1061. doi:10.1038/ncb3195.

123. Herranz N, Gallage S, Mellone M, Wuestefeld T, Klotz S, Hanley CJ, et al. mTOR regulates MAPKAPK2 translation to control the senescence-associated secretory phenotype. Nat Cell Biol. 2015;17(9):1205–1217. doi:10.1038/ncb3225.

124. Wiley CD, Velarde MC, Lecot P, Liu S, Sarnoski EA, Freund A, et al. Mitochondrial dysfunction induces senescence with a distinct secretory phenotype. Cell Metab. 2016;23(2):303–314. doi:10.1016/j.cmet.2015.11.011.

125. Benjamin D, Colombi M, Moroni C, Hall MN. Rapamycin passes the torch: a new generation of mTOR inhibitors. Nat Rev Drug Discov. 2011;10(11):868–880. doi:10.1038/nrd3531.

126. Ridker PM, Everett BM, Thuren T, MacFadyen JG, Chang WH, Ballantyne C, et al. Antiinflammatory therapy with canakinumab for atherosclerotic disease. N Engl J Med. 2017;377(12):1119–1131. doi:10.1056/NEJMoa1707914.

127. Baker DJ, Wijshake T, Tchkonia T, LeBrasseur NK, Childs BG, Van De Sluis B, et al. Clearance of p16Ink4a-positive senescent cells delays ageing-associated disorders. Nature. 2011;479(7372):232–236. doi:10.1038/nature10600.

128. Xu M, Pirtskhalava T, Farr JN, Weigand BM, Palmer AK, Weivoda MM, et al. Senolytics improve physical function and increase lifespan in old age. Nat Med. 2018;24(8):1246–1256. doi:10.1038/s41591-018-0092-9.

129. Song S, Tchkonia T, Jiang J, Kirkland JL, Sun Y. Targeting senescent cells for a healthier aging: challenges and opportunities. Adv Sci (Weinh). 2020;7(23):2002611.

doi:10.1002/advs.202002611.

130. Kirkland JL, Tchkonia T. Cellular senescence: a translational perspective. EBioMedicine. 2017;21:21–28. doi:10.1016/j.ebiom.2017.04.013.

Acknowledgements

This dissertation was completed at the Department of Neurosurgery, Medical Faculty, University Hospital Düsseldorf, Heinrich Heine University Düsseldorf. I am grateful for the opportunity to carry out this work in a research environment that provided both scientific guidance and practical support.

I owe special thanks to my supervisor, Prof. Dr. med. Sajjad Muhammad, for giving me the opportunity to work on this project and for guiding me throughout my doctoral research. His scientific input, critical discussions, and continuous support were essential for the development of this dissertation. I particularly appreciate his trust, patience, and encouragement during the different stages of the project, from experimental design to manuscript preparation. I would also like to express my sincere gratitude to Prof. Dr. med. Majeed Rana for his scientific guidance, constructive advice, and support throughout this doctoral project.

I am also thankful to Prof. Dr. med. Katharina Faust for her support and for providing the academic environment in which this work was conducted. Her contribution to maintaining a productive and supportive research setting at the Department of Neurosurgery is sincerely appreciated. I would like to acknowledge Dr. Dilaware Khan for his valuable help during this project. His technical experience, scientific suggestions, and practical advice were highly important for the progress of my experimental work. I also thank Hongjun Liu and Robert Muhereza for their collaboration, discussions, and support during the preparation of the study.

My appreciation also extends to all colleagues and members of the Department of Neurosurgery who contributed to a constructive working atmosphere. Their help, whether through technical assistance, scientific exchange, or daily support in the laboratory, was an important part of this work. I gratefully acknowledge the financial support from the China Scholarship Council, which made it possible for me to pursue my doctoral research in Germany.

Finally, I wish to thank my family, especially my parents, for their constant support throughout my studies. Their understanding, encouragement, and trust have accompanied me during the challenging and rewarding moments of this doctoral journey. This dissertation would not have been possible without their support.